Economic valuation of subsurface water contributions to watershed ecosystem services using a fully-integrated groundwater–surface water model

Tariq Aziz[1,2,*], Steven K. Frey[1,3], David R. Lapen[4], Susan Preston[5], Hazen A. J. Russell[6], Omar Khader[1,7], Andre R. Erler[1], Edward A. Sudicky[1,3]

[1]Aquanty, 600 Weber St. N., Unit B, Waterloo, ON, N2V 1K4, Canada
[2]Ecohydrology Research Group, Water Institute and Department of Earth and Environmental Sciences, University of Waterloo, Waterloo, N2L 3G1, ON, Canada
[3]Department of Earth and Environmental Sciences, University of Waterloo, Waterloo, N2L 3G1, ON, Canada
[4]Agriculture and Agri-Food Canada, Ottawa Research and Development Centre, Ottawa, Ontario, Canada
[5]Environment and Climate Change Canada, Ottawa, Ontario, Canada
[6]Geological Survey of Canada, 601 Booth St., Ottawa, ON, K1A 0E8, Canada
[7]Department of Water and Water Structural Engineering, Zagazig University, AlSharqia, Egypt

*Correspondence to: Tariq Aziz (taziz@aquanty.com)

Abstract. Water is essential for all ecosystem services, yet a comprehensive assessment and economic valuation of total (overall) water contributions to ecosystem services production using a fully-integrated groundwater-surface water model has never been attempted. Quantification of the many ecosystem services impacted by water demands an analytical approach that implicitly characterizes both subsurface and surface water resources; however, incorporating subsurface water into ecosystem services evaluation is a recognized scientific challenge. In this study, a fully-integrated groundwater–surface water model—HydroGeoSphere (HGS)— is used to capture changes in subsurface water, surface water, and transpiration (green water use), and along with an economic valuation approach, forms the basis of an ecosystem services assessment for an 18-year period (2000-2017) in the 3830 km^2 South Nation Watershed (SNW), a mixed-use but a predominantly agricultural watershed in eastern Ontario, Canada. Using green water volumes generated by HGS and ecosystem services values as inputs, the marginal productivity of water is calculated to be \$0.26 per m^3 (in 2022 Canadian dollars). Results show maximum green water values during the driest years, with the extreme drought of 2012 being the highest at \$424.7 million. In contrast, the green water value in wetter years was as low as \$245.9 million, while the 18-year average was \$338.83 million. Because subsurface water is the sole contributor to the green water supply it plays a critical role in sustaining ecosystem services during drought conditions. This study provides new insight into the economic contributions of subsurface water and its role in sustaining ecosystem services during droughts, and puts forth improved methodology for watershed-based management and valuation of ecosystem services.

1 Introduction

The role of subsurface water (including groundwater and soil moisture) in socio-economic development is widely acknowledged (Foster and Chilton, 2003); however, its ecological contributions are undervalued (Yang and Liu, 2020), despite being fundamental to the control of terrestrial ecological processes (Qiu et al., 2019). Subsurface water

36 supports numerous ecosystem services that range from provisioning to regulating, supporting, and cultural services

37 (Griebler and Avramov, 2015). While infiltration is a driver for subsurface water recharge, subsurface water discharge

38 and vegetation uptake are, in-turn, key fluxes for supporting terrestrial ecosystems (e.g., wetlands, forests, crops, etc.)

39 (Griebler and Avramov, 2015). Subsurface water can provide a buffer against weather stressors on vegetation and

40 aquatic ecosystems and helps to maintain key processes that underpin ecosystem services (Qiu et al., 2019). To date,

41 most ecosystem services research has focused on aboveground factors and processes (e.g., land use change), and very

42 little focus has been given to subsurface water and its influence on terrestrial ecosystem services (Richardson and

43 Kumar, 2017; Qiu et al., 2019). While some previous research (e.g., Booth et al., 2016; Li et al., 2014) has attempted

44 to link subsurface water with land cover, it typically reflects field scale, static environmental conditions (Qiu et al.,

45 2019). Given the challenges with mapping subsurface water resources, the contribution of subsurface water towards

46 terrestrial ecosystem services is not typically quantified, and the economic value of subsurface water contribution to

47 terrestrial ecosystem services is therefore not assessed.

48 While hydrologic ecosystem services studies are common in the literature (Ochoa and Urbina-Cardona, 2017),

49 groundwater-focused ecosystem services assessments are rare. However, groundwater can be an important regulator

50 of watershed hydrologic behaviour and ecosystem health, especially in regions with a shallow water table, such as the

51 Laurentian Great Lakes Region (Neff et al., 2005; Kornelsen and Coulibaly, 2014). In such areas, groundwater acts

52 as a source of soil water (Chen and Hu, 2004). The importance of groundwater has been noted by Griebler and

53 Avramov (2015) in their review of groundwater ecosystem services, where they highlight the direct role it plays in

54 supplying different types of ecosystem services (Millenium Ecosystem Assessment (MEA), 2005); and they stress the

55 need for a better quantitative understanding of groundwater processes in order to protect and manage groundwater and

56 its ecosystem services. Furthermore, Mammola et al. (2019) emphasize that subterranean ecosystems are largely being

57 overlooked in conservation policies. Based on a preliminary assessment of all the regions around the world where

58 groundwater plays a critical role in ecosystem services, and considering that approximately 43 % of consumptive

59 irrigation is sourced from groundwater (Siebert et al., 2010), the lack of focus on subsurface water ecosystem services

60 is not due to lack of need, rather the lack of use of suitable tools to conduct the required analysis.

61 Hydrological models can efficiently and accurately quantify water storages and fluxes over large spatial scales. With

62 groundwater ecosystem services' increasing role in policy-making (Honeck et al., 2021) and sustainable groundwater

63 resources management, new tools are required for their mapping. At present, common modeling tools available for

64 ecosystem services mapping include relatively simple matrix models (i.e., Decsi et al., 2022), and more complex

65 models such as ARtificial Intelligence for Environment & Sustainability (ARIES) (Villa et al., 2021), Co$ting Nature

66 (Mulligan, 2015), Envision (Bolte, 2022), and Integrated Valuation of Ecosystem Services and Tradeoffs (InVEST)

67 (Natural Capital Project, 2022), with InVEST being by far the most prominent in the scientific literature (Ochoa and

68 Urbina-Cardona, 2017). However, ecosystem services specific models, such as the InVEST Water Yield Model, have

69 limited capability to simulate all relevant hydrological processes (Redhead et al. 2016), because their hydrologic tools

70 typically focus on one water compartment and/or are simplified to the point where hydrologically mediated ecosystem

71 services cannot be fully characterized (Dennedy-Frank et al., 2016; Vigerstol and Aukema, 2011). Complete

72 characterization of spatially and temporally varying water storages and fluxes that govern ecosystem services over

73 large spatial scales requires more sophisticated, process-based hydrological models (Sun et al., 2017). Hence, models

74 like SWAT (Arnold et al., 1998) and the Variable Infiltration Capacity (VIC) model (Liang et al., 1994) have been

75 used for hydrologic ecosystem services assessment, however even these models are limited in their ability to simulate

76 complex subsurface water movement and water exchanges between the surface and subsurface. Within the hydrologic

77 modeling community, it is acknowledged that structurally complex, fully-integrated subsurface–surface water models

78 are the current state-of-the-art for capturing the interplay between subsurface and surface water systems across a wide

79 range of spatial scales (Barthel and Banzhaf, 2016; Berg and Sudicky, 2019), however, this class of models, to best of

80 our knowledge, has not yet been applied towards ecosystem services valuation.

81 In humid climates, evapotranspiration is often the most significant component of the hydrologic cycle after

82 precipitation, and must be carefully considered when modelling near surface hydrologic processes. Evapotranspiration

83 is a fraction of rainfall that eventually returns to the atmosphere through evaporation and transpiration (Jin et al., 2017;

84 Condon et al., 2020), which represent large fluxes of both water and energy across the land surface–atmosphere

85 boundary (Tan et al., 2021). Transpiration, a dominant flux in evapotranspiration, results from plant use of green

86 water—the water in the soil available to plants (Casagrande et al., 2021). Thus, green water, by extension, is crucial

87 for ecosystem functioning (An and Verhoeven, 2019), and supporting ecosystem services associated with healthy and

88 productive plant life (Zisopoulou et al., 2022; Schyns et al., 2019). Hence, transpiration serves as a key driver in

89 providing ecosystem services (Liu and El-Kassaby, 2017), and is a fundamental process by which to model/map

90 terrestrial ecosystem services production. The degree of transpiration in an ecosystem is tied to subsurface water

91 available to plants, temperature, wind, light and stomatal controls, for example (Lowe et al., 2022). While specifically

92 capturing the interplay between green water and transpiration rates is complex, the generalized linkage between them

93 is nevertheless useful for valuing green water in supporting ecosystem services provided by transpiring vegetation;

94 and fully-integrated hydrological models that capture subsurface-surface water interactions, will be necessary

95 analytical tools in this regard.

96 Changes in evapotranspiration can influence water availability and ecosystem health at a watershed scale (Zhao et al.,

97 2022). Under drought conditions, subsurface water reserves can become critically important for sustaining plant

98 growth (Condon et al., 2020), and hence, mapping linkages between subsurface water and transpiration is important

99 for sustainable water and ecosystem services management (Yang et al., 2015). Fully integrated subsurface-surface

100 hydrologic models are potentially well suited for such mapping applications. A number of fully-integrated subsurface-

101 surface models have been developed, and benchmarking studies have been conducted wherein select models have

102 been described in detail, and their simulation behavior compared (Maxwell et al., 2014; Kollet et al., 2016).

103 In this study, the HydroGeoSphere (HGS) fully-integrated subsurface–surface water model (Aquanty, 2021; Brunner

104 and Simmons, 2012) is introduced as a tool for mapping hydrological fluxes and water storage fluctuations, and

105 quantifying subsurface water contributions to terrestrial ecosystem services at the watershed scale ($\sim$4000 km^2). In

106 combination with a benefits transfer approach, the results from HGS modelling are extended to an economic valuation

107 of water contributions to ecosystem services. Until now, fully-integrated subsurface-surface models such as HGS have

108 not been widely demonstrated in the scientific literature as tools for modeling ecosystem services, while at the same

109 time, the economic value of subsurface water has been overlooked in ecosystem services valuation assessments.

110 Accordingly, the study improves our understanding of overall hydrologic contributions to ecosystem services.

111 Furthermore, using the HGS model outputs to support the economic valuation of subsurface water contributions to

112 transpiration, and ultimately to terrestrial ecosystem services, is also novel. Hence, this work helps to advance the

113 science of ecosystem service valuation in terms of conceptual, methodological, and quantitative understanding.

114 Results from this study are also directly relevant to the broader scientific and policymaking communities who are

115 seeking insights into the role of subsurface water in supporting societal endpoints under a wide range of different

116 climatological conditions in humid continental climates.

2 Materials and methods

2.1 Study area

This study focuses on the South Nation watershed (SNW), located in eastern Ontario, Canada, with an area of approximately 3,830 km^2 (Fig. 1). The SNW is relatively flat, with approximately 100 m of vertical relief in the land surface (Fig. A1). It is primarily an agriculture-focused watershed, with relatively low population density. The eastern flank of the city of Ottawa encroaches on the Northwest corner of the watershed. The SNW surface water flow network is approximately 6,489 km long and consists of 1,606 km of Strahler order 3+ (relatively large), 1,548 km of Strahler order 2, and 3,335 km of Strahler order 1 (smallest) waterways (Fig. A2). Many of the low order features are either manmade agricultural drainage ditches or straightened natural watercourses designed to drain the agricultural landscape.

Soil drainage conditions across the watershed are generally imperfect, poor, or very poor (Fig. A3), with some pockets are considered as well drained (Soil Landscapes of Canada Working Group, 2010). The wide extent of poorly drained soils in the SNW necessitates subsurface tile drainage for crop production. Tile drainage is employed widely in the watershed to enhance agricultural productivity and to facilitate cropping activities (Fig. A4). Across most of the SNW the soils are primarily underlain by glacial, fluvial, and colluvial Quaternary deposits (Ontario Geological Survey, 2010). These sediments are composed of sand, silt, clay, gravel, and glacial till, and range in thickness from 0 m to approximately 90 m across the watershed. Eight soils have been identified in the SNW (Soil Landscapes of Canada Working Group, 2010), mainly composed of clay loam and sandy loam textures (Fig. A3 (a)). Localized incised bedrock channels and Quaternary esker deposits (Cummings et al., 2011) are important sources of groundwater for both ecological function and human/livestock supply, and most of the rural residents in the SNW rely on groundwater for domestic and farm use.

The SNW is characterized by relatively wet temperate climate with cold winters and warm summers. The annual average temperature is just over 5 C, with average summer highs reaching 26°C in July and average winter lows reaching -14°C in January (https://climate.weather.gc.ca/climate_normals). Present day landcover is given in Fig. 1.

141
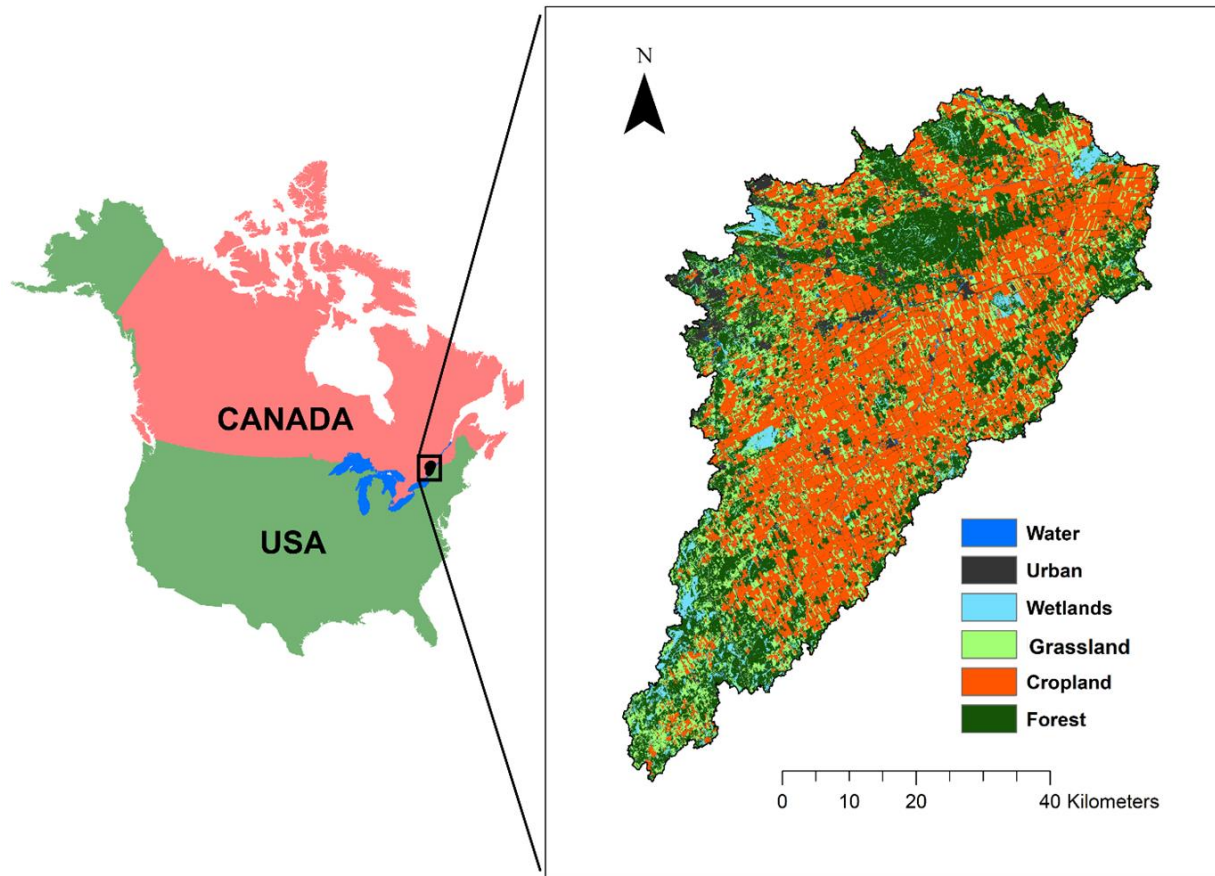
Figure 1: Location of the South Nation Watershed (SNW) in North America. The inset figure (right) shows the land use distribution across the SNW.

2.2 Water balance quantification with HydroGeoSphere (HGS)

The water balance strongly influences ecosystem functions and the associated ecosystem services, as it governs both abiotic and biotic processes occurring within ecosystems (Mercado-bettín et al., 2019). Consequently, evaluating the role of water towards ecosystem services supply necessitates an analysis capable of water balance partitioning (i.e., disaggregation of the water balance into its fundamental components such as precipitation, subsurface evaporation, transpiration, surface and subsurface storages) (Casagrande et al., 2021). As HGS is a dynamic fully-integrated subsurface–surface hydrologic model, it generates time varying simulation outputs for all components of the terrestrial hydrologic cycle (Fig. 2), thus alleviating a common limitation of ecosystem services models in that they do not account for transient behavior (Vigerstol and Aukema, 2011). HGS employs a physically based approach to simulate

153 water movement and the partitioning of precipitation input into surface runoff, streamflow, evaporation, transpiration,

154 groundwater recharge, as well as groundwater discharge into surface water bodies like rivers and lakes (Brunner and

155 Simmons, 2012). Furthermore, HGS outputs can also be generated for the entire model domain (i.e., the watershed)

156 or refined for smaller spatial scales such as subwatersheds, with the downscale limit being that of an individual finite

157 element within the finite element mesh (FEM).
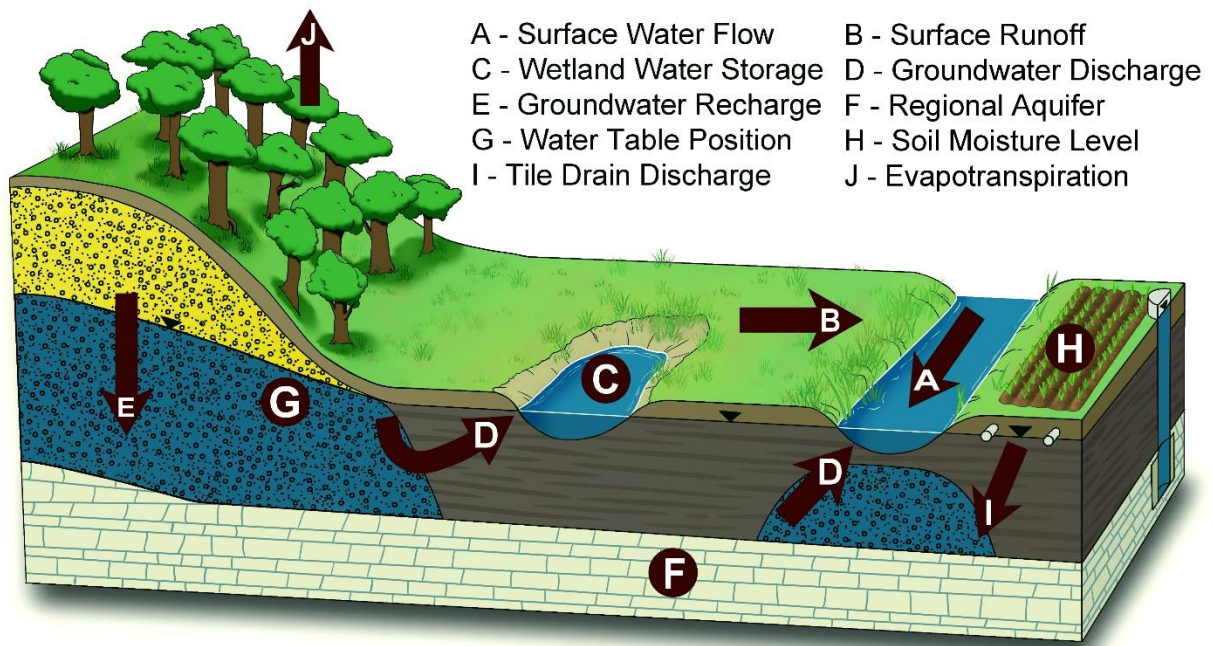
158

159 **Figure 2: Key components of the terrestrial hydrological cycle captured in HGS models over a range of spatial**

160 **scales.**

161 It should be noted that the fidelity of the HGS outputs is also dependent on the model scale, with large scale models

162 generally having lower spatial resolution than small scale models as a result of computational constraints, and in some

163 cases, data constraints. For example, a model of a 766,000 km^2 river basin (e.g., Xu et al., 2021a)) is best suited to

164 answer big picture questions (i.e., basin water balance), while a model built at similar scale to the SNW (e.g., Frey et

165 al., 2021)) can be used to address questions pertaining to more localized processes (i.e., individual wetland influences,

166 groundwater recharge and discharge patterns, aquifer conditions, and soil moisture conditions). If even more localized

167 insights are required, HGS models can be constructed for field or plot scale domains (up to approximately 10 km^2),

168 where questions pertaining to things such as riparian zones, soil structure, manure application, and tile drainage

169 influences on both water quantity and quality can be evaluated (Fig. 2). Thus, HGS is a scalable and robust model for

170   ecosystem services analysis across a range of different spatial scales and different levels of hydrologic process detail.

171   For the SNW, HGS is used to simulate watershed surface water outflow, transpiration (green water), subsurface water

172   storage, and land surface water storage (reflecting water held in wetlands and reservoirs) using the model construction

173   framework presented in Frey et al. (2021).

174   **2.2.1 Model construction**

175   **2.2.1.1 Finite Element Mesh (FEM)**

176   The HGS model utilizes a 3-D unstructured FEM that extends across the full 3830 km^2 area of the SNW. The 1-D

177   river/stream channel features, 2-D overland flow domain (reflecting land surface topography), and 3-D subsurface

178   flow domain (reflecting hydrostratigraphy) all share the same mesh geometry, with the 1-D and 2-D domains sharing

179   common coordinates with the 3-D domain across the top surface of the model. The FEM for the SNW model resolves

180   all Strahler 2+ stream/river features as mesh discretization control lines, with element edge length maintained at 100

181   m, while away from the control lines the element edge lengths extend up to 300 m. The FEM contains layer surfaces

182   that correspond to hydrostratigraphic surfaces, with each individual layer consisting of 171,609 finite elements.

183   Accordingly, over the eight model surfaces (seven subsurface layers); the FEM contains 1,201,263 3-D finite elements.

184   **2.2.1.2 Hydrostratigraphy**

185   The seven subsurface layers represent (from the top down) three soil layers, three Quaternary hydrostratigraphic

186   layers, and one bedrock layer. The soil layers extend from 0–0.25 m, 0.25–0.5 m, and 0.5–1 m depth relative to the

187   top surface, which is defined with the Ontario Integrated Hydrology Data digital elevation model

188   (https://geohub.lio.gov.on.ca/maps/mnrf::ontario-integrated-hydrology-oih-data/about). The hydraulic properties for

189   the soil layers vary spatially according to the soil polygons defined in the Soil Landscapes of Canada (SLC, Soil

190   Landscapes of Canada Working Group, 2010), and are defined in two steps as follows: (1) properties extracted from

191   SLC are used in conjunction with the Rosetta pedotransfer functions (Schaap et al., 2001) to obtain estimates for

192   hydraulic conductivity, water retention and relative permeability, residual saturation, and porosity parameters, and (2)

193   hydraulic conductivity, water retention and relative permeability parameters are subsequently tuned during model

194   calibration. The three Quaternary layers are of variable thickness, where the interface surfaces represent lithology

195   contrasts derived from a simplified version of the 3-D geological model produced for the SNW by Logan et al. (2009).

196   Hydraulic properties for the Quaternary materials are assigned based on lithology. Underlying the Quaternary layers

197 is a single hydrostratigraphic layer with uniform hydraulic conductivity representative of the Phanerozoic bedrock.

198 When assembled, the model layers depict a 3-D subsurface realization of the SNW hydrostratigraphy (Fig. 3).
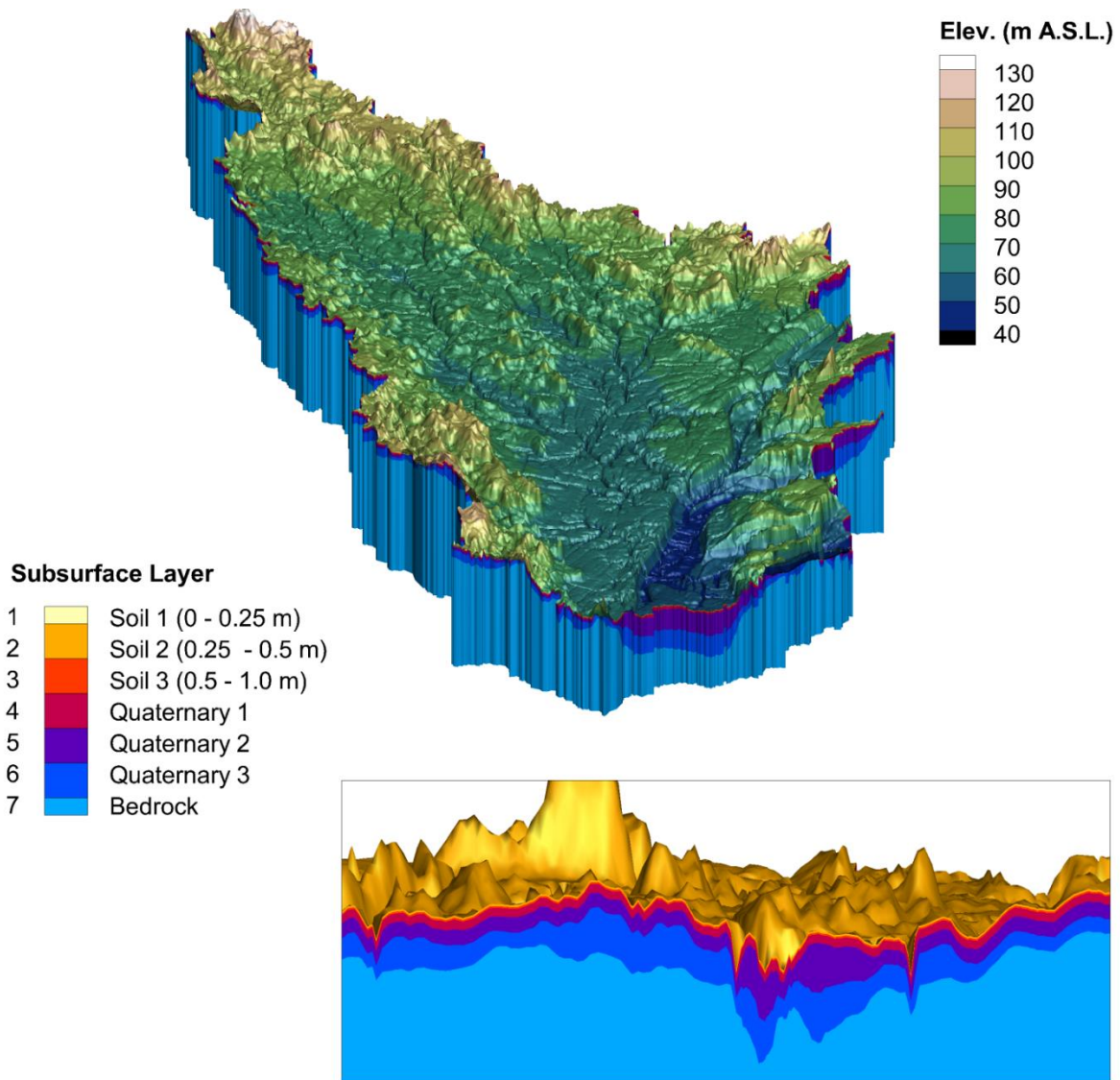
199

200 **Figure 3: Three-dimensional perspective of the South Nation HydroGeoSphere model, and the**

201 **hydrostratigraphic layering (inset). Note the 100x vertical exaggeration.**

202 **2.2.1.3 Land surface configuration**

203 The land surface in the HGS model represents land cover distribution defined by the gridded, 30 m resolution, 2017

204 Annual Crop Inventory dataset (Agriculture and Agri-Food Canada, 2022) simplified to six categories (water, urban,

205 wetland, grassland, cropland, and forest). Root depth for the cropland (1 m), forest (2.9 m), wetland (1 m), grassland

206 (2.1 m), and urban (1 m) landcovers was held static over the simulation interval. Spatially distributed leaf area index

207 (LAI) is a transient parameter defined with the 8-day composite, 500 m resolution MOD15A2H v006 data product

208   (Myneni et al., 2021). Each landcover category utilizes a unique surface roughness (Manning's *n* coefficient) value,

209   ranging from 0.001 (urban) to 0.03 s/m$^{1/3}$ (forest). Land cover properties, as well as subsurface hydraulic properties,

210   were mapped into the HGS model's unstructured FEM using a dominant component approach, such that when two or

211   more property classes exist within the input data set for a single finite element, the majority class is represented.

212   **2.2.1.4 Climatology**

213   Time-varying and spatially distributed climate data with daily temporal resolution liquid water influx (LWF) and

214   potential evapotranspiration (PET) is used to force the HGS model for the 2000 to 2018 simulation interval. LWF is

215   derived from precipitation obtained from McKenney et al. (2011) in combination with snow water equivalent (SWE)

216   estimates from the ERA5-Land land-surface reanalysis (Muñoz-Sabater et al., 2021), where LWF is the sum of liquid

217   precipitation (rain) and snowmelt (daily changes in SWE).

218   Potential evapotranspiration primarily depends on the surface radiation budget, temperature, humidity, and near-

219   surface wind speed (Allen et al., 1998); however, of these variables, only minimum and maximum temperature are

220   readily available for the full SNW. Hence, PET forcing for the SNW model is calculated with the Hogg method (Hogg,

221   1997), which is consistent with Erler et al. (2019) and Xu et al. (2021), who both reported good agreement with the

222   observed water balance in the Great Lakes region when using the Hogg method. The Hogg method is based on the

223   FAO Penman-Monteith approach (Allen et al. 1998) with a simplification that involves the radiation budget and

224   humidity approximated as a function of daily minimum and maximum temperature, and wind speed assumed to be

225   constant.

226   **2.2.2 Model performance evaluation**

227   The SNW HGS model was run continuously for the 2000–2017 with daily temporal resolution climate forcing, and

228   simulation performance is evaluated using observed surface water flow rates and groundwater levels. The observation

229   data is derived from daily temporal resolution surface water flow monitoring conducted at nine Water Survey of

230   Canada (WSC) hydrometric stations (Figure 4a) and groundwater level data from 10 Provincial Groundwater

231   Monitoring Network wells that was collected hourly but aggregated into daily average values (Figure 4b). The Nash-

232   Sutcliffe Efficiency (NSE) and Percent Bias (Pbias) metrics (Moriasi et al., 2007) are used to evaluate surface water

233   flow simulation performance, while the coefficient of determination (R^2) and root mean square error (RMSE) is used

234   to evaluate groundwater simulation performance. It should be noted that groundwater pumping is not represented in

235 the model as it is deemed to be a very minor component of the overall water balance, and because it is extremely

236 difficult to characterize and simulate at the scale of the SNW.
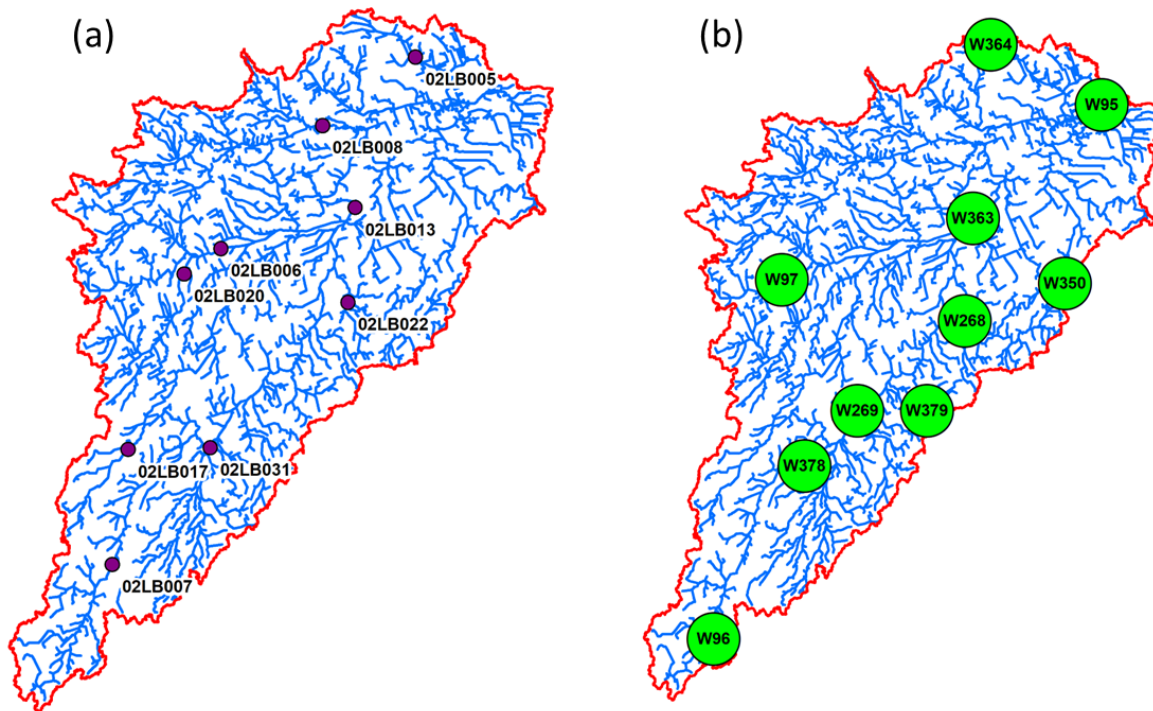
237

238 **Figure 4: Distribution of (a) Water Survey of Canada surface water flow gauges, and (b) Provincial**

239 **Groundwater Monitoring Network wells across the South Nation watershed.**

240 **2.3 Ecosystem services water productivity**

241 The benefit transfer method is used to derive the unit values of ecosystems in the SNW. The benefit transfer method,

242 which is a widely used technique for assessing the economic value of ecosystem services, relies on secondary data

243 obtained through the implementation of various other economic valuation methods (Aziz, 2021). The benefit transfer

244 method, widely used for the economic valuation of ecosystem services, leverages existing valuation studies to estimate

245 the value of the services in different geographical contexts. The method relies on two key assumptions. First, it

246 assumes that the value of any ecosystem service (or bundle) under valuation is comparable across different regions,

247 which may not always hold true due to variations in ecological and socio-economic conditions. Additionally, the

248 methods used in the primary studies (e.g., market price, replacement cost methods) assume that market prices or the

249 costs of replacing ecosystem services accurately reflect their true value (Aziz et al., 2023). These assumptions

250 inherently limit the precision of the results, meaning the estimated values should be interpreted as approximate rather

than definitive. Nevertheless, these estimates provide useful insights, especially for regions like the South Nation Watershed, where primary valuation studies are lacking and can guide initial policy development and resource management decisions.

A study conducted approximately 65 km from the SNW in the Ottawa-Gatineau region, by L'Ecuyer-Sauvageau et al. (2021), assembles the values for 13 ecosystem services: agricultural services, global climate regulation, air quality, water provision, waste treatment, erosion control, pollination, habitat for biodiversity, natural hazard prevention, pest management, nutrient cycling, landscape aesthetics, and recreational activities. These 13 ecosystem services are the focus of the present analysis and their unit values have been correspondingly generated by major ecosystems using market price, replacement cost, and benefit transfer methods. The unit values for ecosystem services are based on similarities in ecologic and socio-economic conditions between the studied and policy sites, and converted using the purchasing power parity (L'Ecuyer-Sauvageau et al., 2021). The benefit transfer method provides an approximation of ecosystem service values with potential transfer errors ranging from 62% to 86% based on domestic studies (Aziz, 2021). In our study context, we transfer the values from the region immediately adjacent to our study region, an approach that constrains the error. After adjusting these values for inflation, the value of ecosystem services in the SNW is calculated using the following equation.

$$EV_t = \sum_{k=1}^{n}(A_k \times UV_k) * VI \qquad (1)$$

EV_t = Value of ecosystem services for year t

A_k = Area of land use k

UV_k = Unit value of ecosystem services for land use k

VI = Vegetation indicator, a ratio of yearly to average net primary production (NPP) = NPP_{year}/NPP_{mean}

We use net primary production as an indicator to characterize the vegetation vigor (Xu et al., 2012) and to adjust the values of ecosystem services over time in the SNW. The Moderate Resolution Imaging Spectroradiometer (MODIS) (https://appeears.earthdatacloud.nasa.gov/) NPP data (at 500m resolution) for the 2000 to 2017 study period is used (Fig. A5). Using the ArcGIS Spatial Analyst Toolbox, yearly mean NPP values are calculated (Table 2). The average ecosystem services water productivity is then calculated using ecosystem services values and productive green water volumes (i.e., transpiration) in equation 2:

$$V_{Wt} = (EV_t)/(X_{wt}) \qquad (2)$$

V_{wt} is the average product of water ($ per m^3), X_{wt} is the total volume of water transpired (or volume of green water used for transpiration) in a year 't'.

280   **2.4 Valuation of subsurface water contribution towards ecosystem services supply**

281   A water production function is developed using economic values of the supply of the 13 watershed ecosystem services

282   over the 18-year study period and corresponding volumes of green water used by plants for transpiration. Because

283   ecosystem services value is proportional to vegetative biomass production (Costanza et al., 1998), the values are

284   modified over time using relative changes in ecosystem vegetative biomass in the watershed (Xu and Xiao, 2022).

285   The slope of the production function represents the ecosystem services marginal water productivity (MP_w). HGS

286   model outputs capture the volume of subsurface water contributing to transpiration. Using transpired water volume

287   and MP_w, the economic value of green water is calculated (Eq.3).

$$V_t = X_{wt} * MP_w \qquad (3)$$

289   Where V_t is the value of subsurface water used towards ecosystem services supply, X_{wt} is the volume of subsurface

290   water transpired or productive green water volume in year 't', and MP_w is the marginal productivity of water.

291   **3 Results**

292   **3.1 HGS outputs**

293   For the 2000 to 2017 simulation interval, the HGS model reproduces surface water flow rates at the nine WSC

294   hydrometric stations across the SNW with good accuracy per the interpretation guidance provided by Moriasi et al.

295   (2007). Based on daily evaluation frequency, NSE at the individual gauge stations ranges from 0.59 to 0.70, with a

296   mean of 0.66; while PBias ranges from -17.4 % to 17.1 %, with a mean of 3.9 % (Fig. 5). Groundwater levels were

297   also reproduced across the SNW with reasonable accuracy for the 2000 to 2017 interval. The R^2 between simulated

298   and observed water levels in the 10 observation wells is 0.98, with the simulated values having a mean value 2.8 m

299   higher than the observed values. Groundwater simulation performance at the individual wells is presented in Table 1.

300   HGS outputs (Fig. 6) also include total watershed surface water outflow, ET_a rates (based on subsurface transpiration

301   and evaporation, surface evaporation and canopy evaporation), subsurface water storage (groundwater storage plus

302   soil moisture storage) and land surface water storage. During the simulation period, transpiration accounts for a

303   substantial proportion of ET_a, ranging from 45% to 65% (Table A1). Consequently, it emerges as the dominant process

304   contributing to the overall ET_a. As evident in Fig. 6, water storage volumes fluctuate over inter- and intra-annual time

305   frames, with the most notable decline in storage aligned closely with the drought in 2012.

306
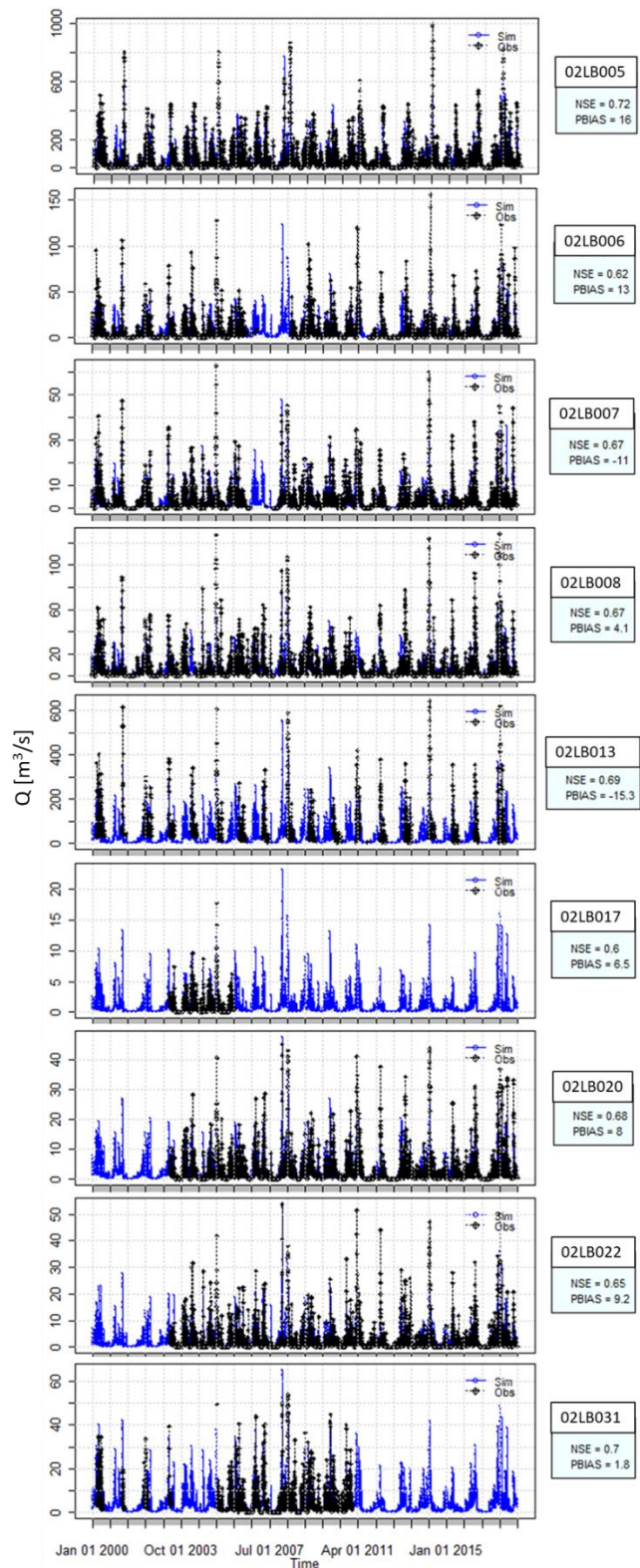
Figure 5: Simulated vs. observed surface water flow rates at the nine Water Survey of Canada (WSC) flow gauges incorporated into the model calibration process, along with Nash-Sutcliffe Model Efficiency (NSE) and Percent Bias (PBias in %) performance metrics. Note that not all gauges have a full data record over the 18-year simulation interval.

310 **Table 1. For the 10 monitoring well locations, observed vs. simulated average groundwater head, and root mean square**
311 **error between daily temporal resolution observed and simulated head, over the 2000 – 2017 simulation interval.**

Well	Observed Average Head (mASL)	Simulated Average Head (mASL)	RMSE (m)
95	48.2	62.0	13.8
96	99.1	99.1	0.8
97	84.9	86.9	2.1
268	72.4	72.3	0.5
269	68.4	70.9	2.7
350	111.3	109.5	2.1
363	57.4	61.6	4.2
364	43.2	50.3	7.2
378	74.7	77.0	2.4
379	89.4	87.4	1.9

312

313
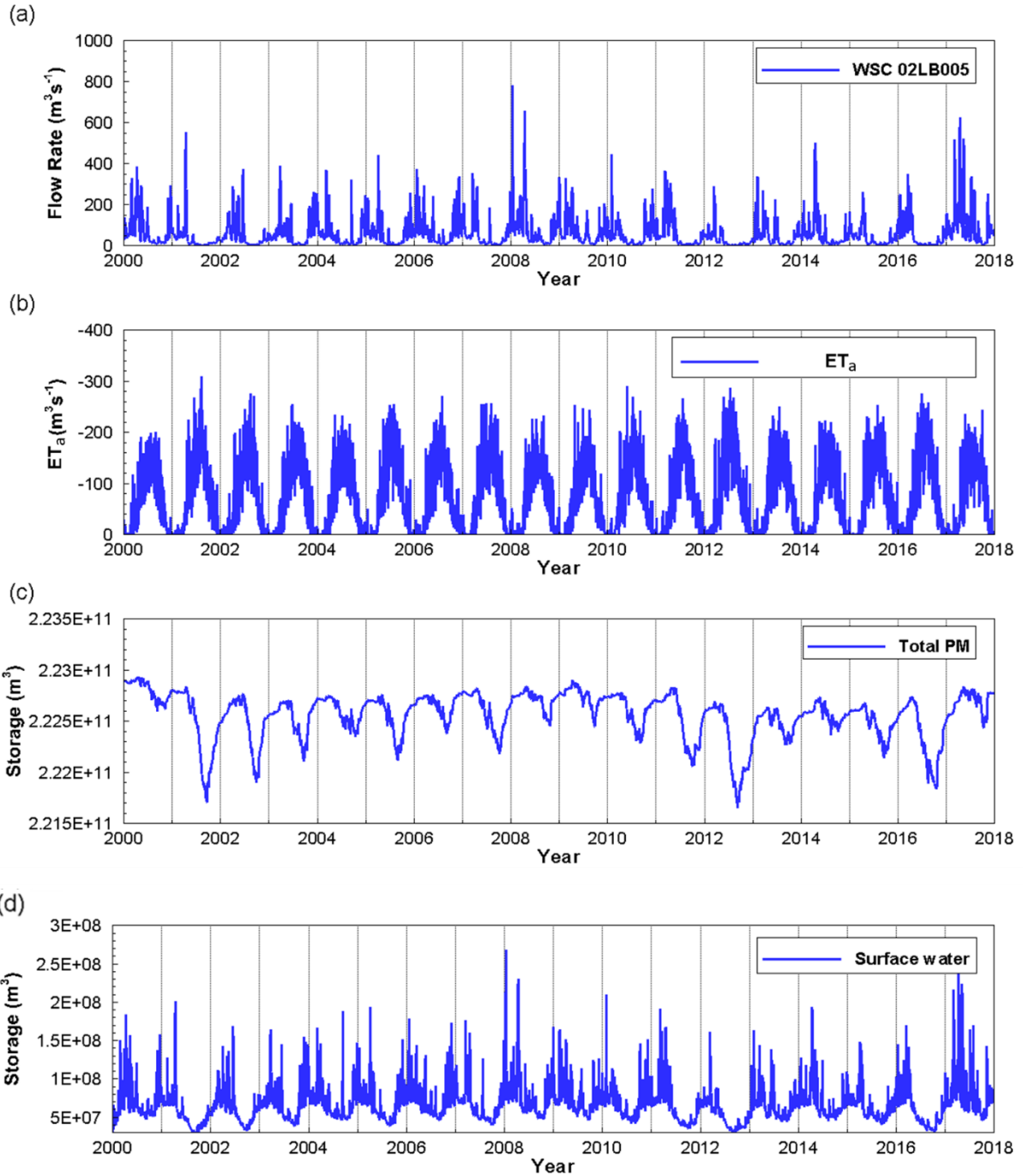
Figure 6: Time series outputs from the South Nation watershed HydroGeoSphere (HGS) simulation over the 2000-to-2017-time interval. (a) stream flow at the furthest downstream hydrometric station, (b) watershed evapotranspiration, (c) watershed subsurface water storage, and (d) watershed land surface water storage.

The HGS output was generated at variable time steps that were each no larger than 1 day, and then aggregated to yearly values for use in the ecosystem services assessment (Table A1). Annual deviations from the long term mean, for ET_a, transpiration, total precipitation, and surface and subsurface water storage, are presented in Fig. 7. In the

320 context of subsequent analysis and discussion, it should be noted that the drought year of 2012 exhibits the highest

321 ET_a and transpiration, lowest precipitation, and largest relative drops in both subsurface and surface water storage.

322
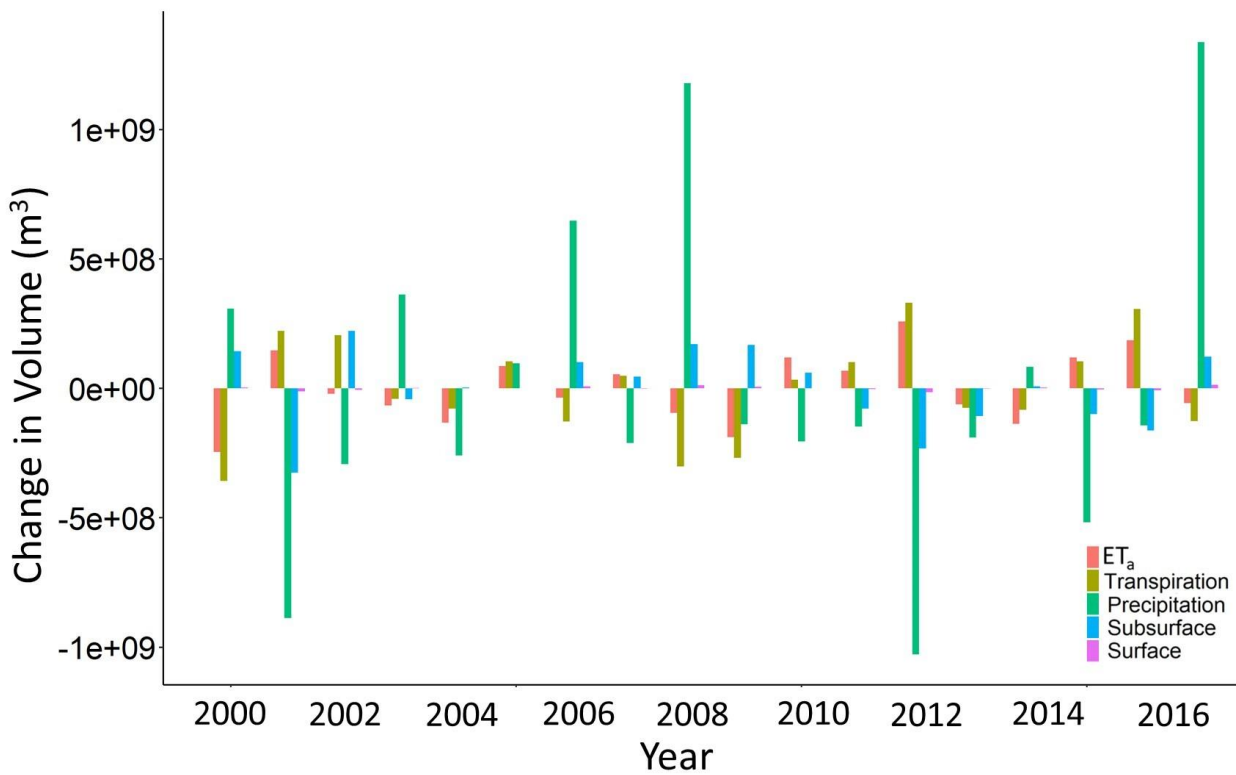
Figure 7: Annual deviation from the long term (2000-2017) mean evapotranspiration (ET_a), transpiration, precipitation, and subsurface and surface water storages.

3.2 Valuation of ecosystem services, and average and marginal water productivity

Table 2: Land use types and unit values of ecosystem services for the SNW.

Land Use	Area (hectare)	Unit value ($/hectare/year)
Water	1,299	165
Urban	25,734	1,177
Wetlands	16,709	71,273
Grasslands	76,961	4,152
Croplands	154,810	1,666
Forest	107,470	4,993

327

328 Using unit values for the major land use types in the SNW (Table 2) and land use area, total value of the 13 ecosystem

329 services under consideration is $2.33 billion per year (in CAD 2022) prior to further annual modifications based on

330 the vegetation indicator (Eq. 1). The estimates for average product of water are point estimates based on the value of

331 ecosystem services and productive green water volume (i.e., transpiration) for the corresponding year. Annual NPP

332 data (rescaled between 0 and 1), ES values, transpiration volume, and average water product in the SNW are given in

333 Table 3.

334 **Table 3: Mean Net Primary Production (NPP), ecosystem services (ES) values, transpiration volume, and**

335 **average product of water for the SNW over the 18-year study interval.**

Year	Mean NPP	ES Value (x10^9 $/year)	Transpiration (x10^9 m^3)	Average product of water ($/m^3)
2000	0.59	2.26	0.95	2.39
2001	0.65	2.49	1.53	1.63
2002	0.6	2.30	1.51	1.52
2003	0.6	2.30	1.26	1.82
2004	0.62	2.37	1.22	1.94
2005	0.63	2.41	1.41	1.71
2006	0.58	2.22	1.18	1.89
2007	0.63	2.41	1.35	1.78
2008	0.6	2.30	1.00	2.29
2009	0.58	2.22	1.03	2.14
2010	0.64	2.45	1.34	1.83
2011	0.6	2.30	1.40	1.63
2012	0.63	2.41	1.63	1.48
2013	0.58	2.22	1.23	1.81
2014	0.59	2.26	1.22	1.85
2015	0.65	2.49	1.41	1.77
2016	0.6	2.30	1.61	1.43
2017	0.59	2.26	1.18	1.92

336

337 For the ecosystem services marginal water productivity, a production function is developed using transpiration and

338 ecosystem services values for the SNW (Fig. 8) and the slope of the function equates to the marginal productivity of

339 water, which is $0.26/m^3.

The figure shows a scatter plot with the equation:

$$y = 2 \times 10^{+9} + 0.26\, x$$
$$R^2 = 0.32$$

x-axis: Transpiration (m³/year)
y-axis: Value of Ecosystem Services ($/year)

340
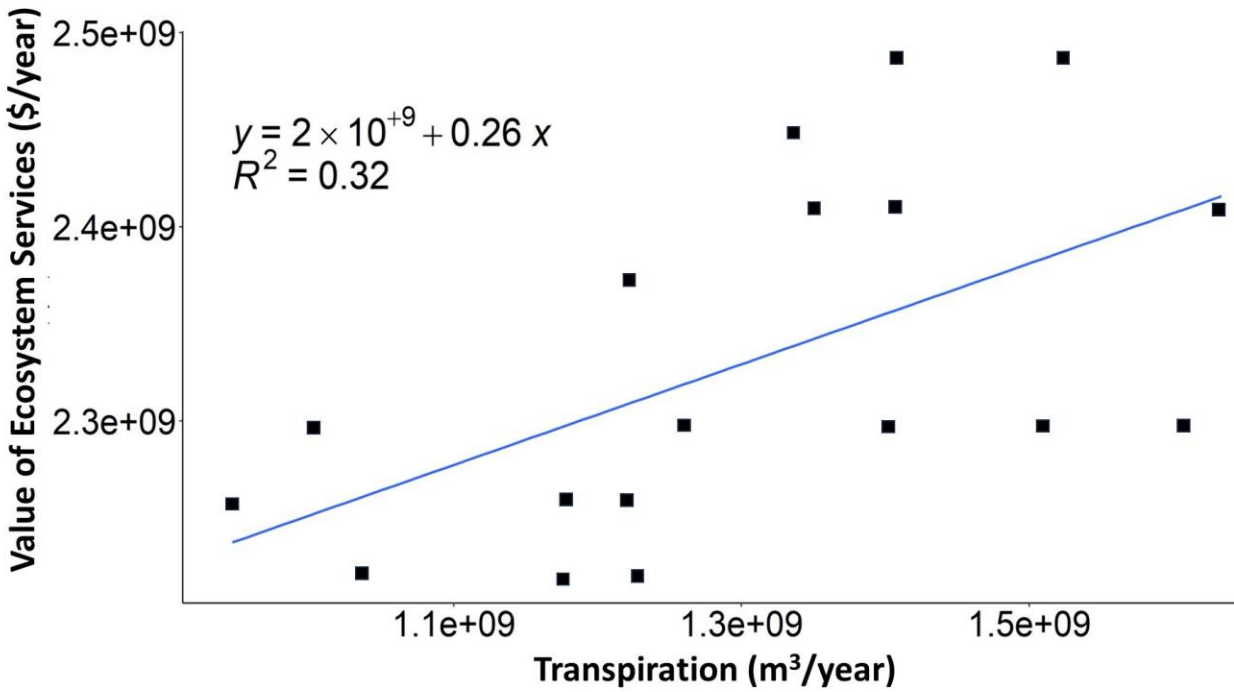
Figure 8: Ecosystem services water production function for the SNW.

To assess the contribution of subsurface water towards ecosystem services, the average ecosystem services water productivity at the watershed scale is calculated (Table 3). The average product of water over the 18 year study interval ranges from \$1.43-2.39 per m³ (Fig. 9). During the drier years (2001-2002, 2012 and 2016), the average product of water declines to local minima. This is because the average product depicts water use efficiency, with the highest value observed for year 2000 indicating that hydrologic conditions favoured the maximum production of ecosystem services with the lowest water consumption in that year.
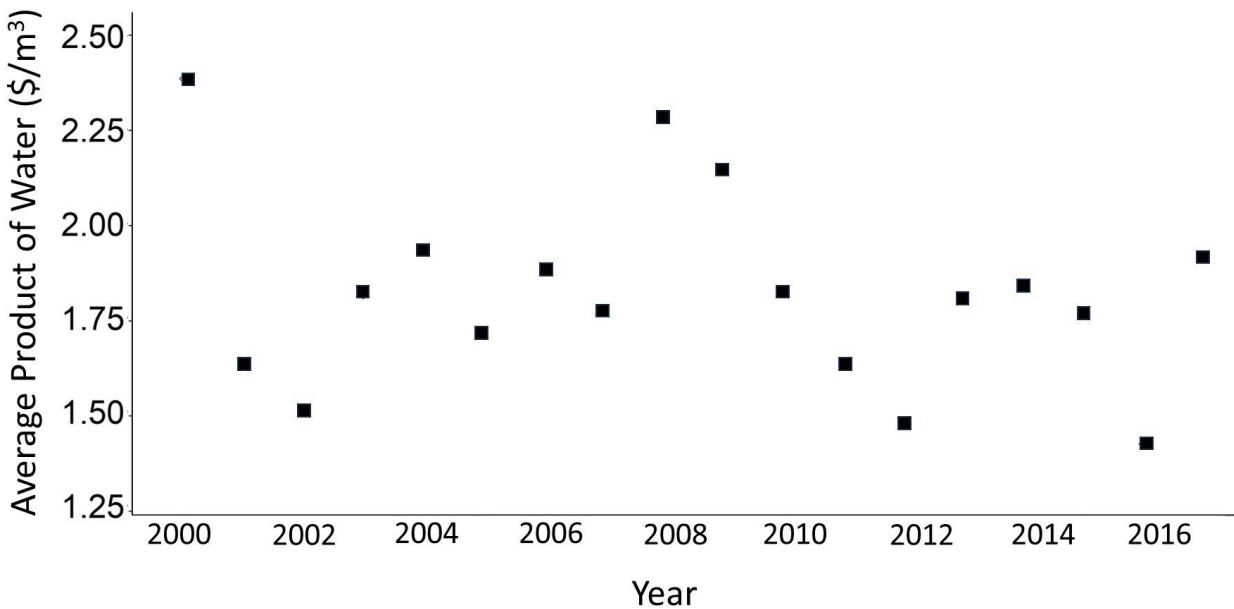
348

349 **Figure 9: Average annual product of water (Table 3) for ecosystem services in the SNW over the 18-year study**

350 **period.**

351 **3.3 Valuation of green water**

352 Using the marginal water productivity and transpiration in the SNW, the value of the productive green water (i.e.,

353 subsurface water) over the study period was calculated (Fig. 10). The annual values range from \$245.9 (year 2000) to

354 \$424.7 (year 2012) million per year, with an overall average of \$338.83 million. In the SNW, precipitation is the main

355 driver of the terrestrial hydrologic cycle and low precipitation is the primary indicator of climatological drought. In

356 general, there is a strong inverse correlation between total annual precipitation and green water value, with an R^2 of

357 0.45 (p <0.0001).

358
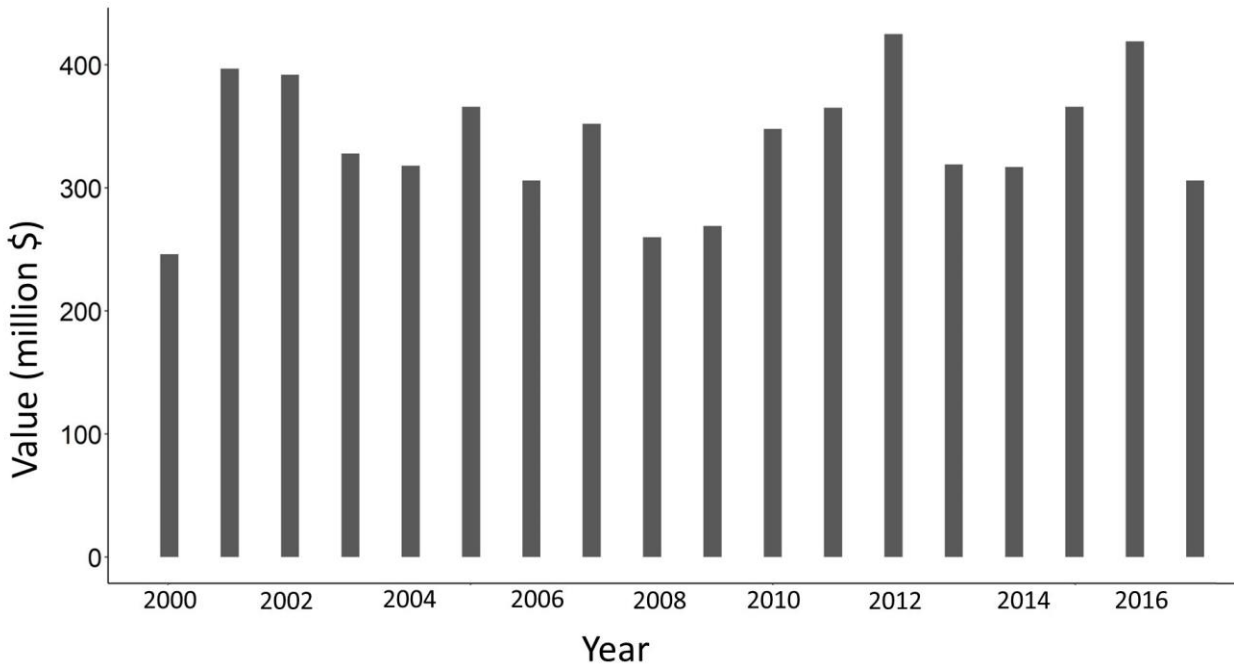
Figure 10: Value of productive green water in the SNW over the 18-year study period.

4 Discussion

4.1 Drought Year Hydrologic Behavior

In the study herein, HGS is used to capture the contributions of subsurface water storage to transpiration (i.e., productive green water) and quantify its role in sustaining transpiration and subsequent ecosystem services.

The annual deviations from the long-term means (Fig. 7) show that ET_a and transpiration are supported by the subsurface and surface storages during droughts. In the drought period from 2001-2002, an interesting situation arises. In 2001, both ET_a and transpiration exhibit positive values relative to the mean. However, in 2002, despite ET_a being negative, transpiration remains positive and surpasses the mean value. This deviation can be attributed to the diminished availability of surface water, leading to reduced evaporation and subsequently lower ET_a. Nevertheless, transpiration continues to exceed the average due to its reliance on subsurface water availability within the SNW. This finding is further supported by previous studies, which suggest that transpiration dominates ET_a during drought years, while evaporation takes precedence during wet years (Zhang et al., 2019). To further compare the fluctuations in different storage zones on a common scale, the standard scores (that is, the change in a storage/standard deviation) for each zone are calculated over time (Fig. 11). The standard scores show that ET_a is supported by both surface and

374 subsurface water storages during the dry periods. However, the contribution of subsurface water by volume during

375 drought is much larger than that of surface water, thus highlighting the important role of subsurface water in supporting

376 transpiring biota during droughts.
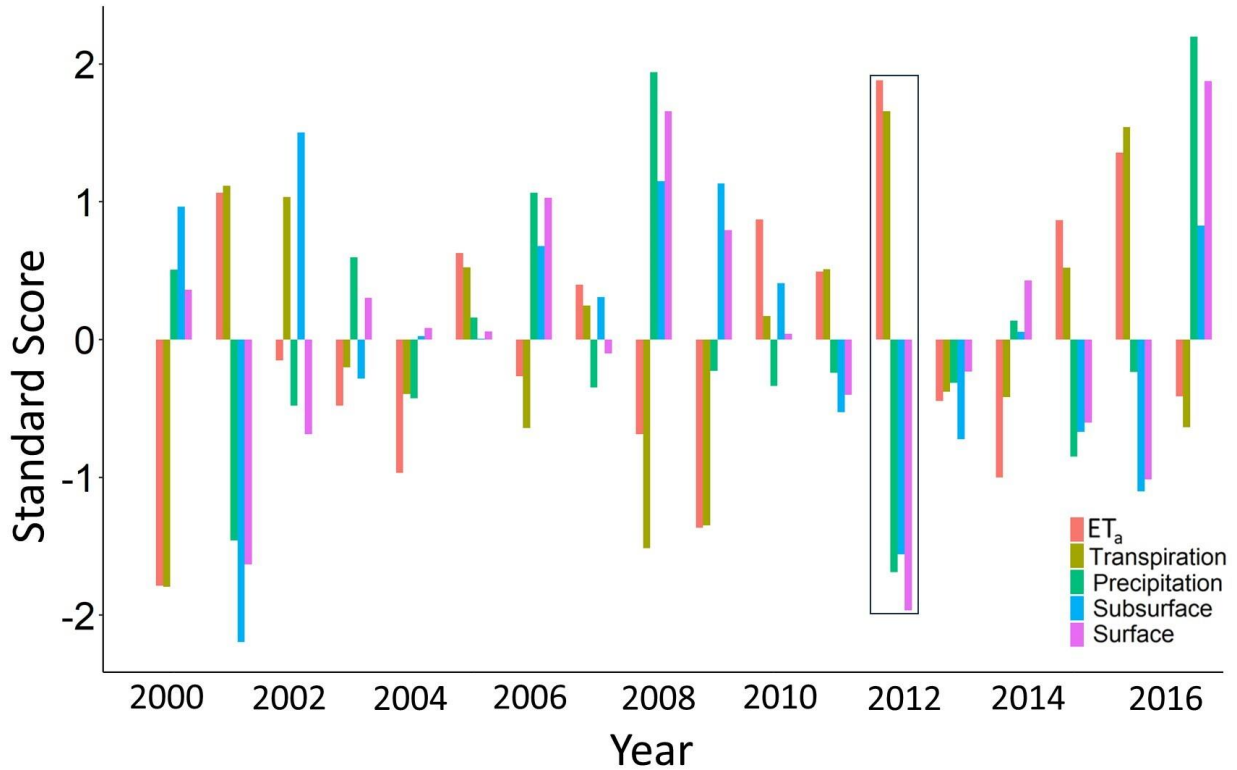
377

378 **Figure 11: Change in standard scores of water storages/hydrological variables over the 18-year study period.**

379 **The scores for the 2012 drought year are bordered.**

380 Comparison of years 2001 and 2012 (both with less precipitation than the 18-year mean) shows that the ET_a was less

381 but outflow was more in 2001 relative to 2012 (Fig. 6(a)). In such case, it is the subsurface water contribution in 2001

382 that maintained the higher surface water flows, which highlights the important role of antecedent conditions in

383 regulating low flow response. Nevertheless, the influence of subsurface water on consumptive water use also depends

384 on the timing of precipitation along with other climatic conditions (e.g., temperature, atmospheric moisture demand,

385 etc.) in the corresponding years (Zhao et al., 2022). During drought periods, vegetation and atmospheric moisture

386 demand is often not met, thus resulting in ecosystem stress along with depletion of subsurface and surface water

387 storages (Zhao et al., 2022). Given the complexities involved with linking transpiration with subsurface water storages,

388 full characterization of transpiration influences on ecosystem services during droughts has until now received little

389 attention.

390   The study quantifies subsurface water ecosystem services values, at the scale of a 3830 km^2 watershed, over a period

391   that encompasses a wide range of climatological conditions. Previous studies (e.g., Loheide, 2008; Su et al., 2022)

392   have estimated groundwater contribution to evapotranspiration by linking water table fluctuation with changes in

393   evapotranspiration. However, over large areas, using water table fluctuation can be complicated by other subsurface

394   water sinks, including deeper groundwater recharge and discharge into surface water receptors. With the HGS

395   approach employed herein, the computed subsurface water evaporation and transpiration, and surface water

396   evaporation, in conjunction with the other hydrologic flow processes depicted in Fig. 2, provides a physical based

397   numeric characterization of water storage contributions to ET_a.

398   The fluctuations in water storages show that, in general and with respect to longer term mean conditions, subsurface

399   water storage repletes when ET_a is negative and depletes when ET_a is positive. In both the 2001 and 2012 drought

400   years, ET_a is relatively high in comparison to the wet years with high precipitation. ET_a in drought years is primarily

401   supported by the drawdown (by volume) in subsurface water storage below the mean level. In general, fluctuations in

402   subsurface water storage across the 18 years are congruent with changes in precipitation, with above-average

403   precipitation aligned with increases in subsurface water storage and vice-versa. In contrast, increased ET_a leads to a

404   reduction in subsurface storage and vice-versa. Over the 18 year study period, the maximum increase in subsurface

405   water storage occurred in the year 2002, immediately following the 2001 drought which had implications far beyond

406   just the SNW (Wheaton et al., 2008). Even though 2002 was a year with less than average precipitation, the drought-

407   impacted subsurface storage conditions led to an antecedent condition across the SNW that was favourable for

408   subsurface water recharge.

409   **4.2 Hydrologic Influences on Ecosystem Services and Economic Valuation**

410   Based on the study herein, fully-integrated groundwater – surface water models, such as HGS, have potential to

411   facilitate better management of watershed scale (approximately 4,000 km^2) water resources for ecosystem services

412   endpoints, as well as help determine the role of a range of water resources that sustain green water supply. A water

413   production function was developed using total green water volumes and total values of 13 ecosystem services in the

414   SNW: agricultural services (net benefits from the crops or agricultural products), global climate regulation, air quality,

415   water provision, waste treatment, erosion control, pollination, habitat for biodiversity, natural hazard prevention, pest

416   management, nutrient cycling, landscape aesthetics, and recreational activities. The ecosystem water production

417   function yields a marginal value of $ 0.26 per m^3 of green water devoted to transpiration (Fig. 8). Globally, Lowe et

418   al. (2022) estimated the average marginal product of water specifically for crop production at $0.083 per m^3. While

419   water productivity is greatest when the smallest amount of water is used/consumed, it also produces the smallest value

420   of ecosystem services at this point. Between 2000 and 2017, transpiration in the SNW is highest during the driest

421   years (Zhao et al., 2022). The NPP does not decline during these periods, likely due to enough subsurface water to

422   meet plant demands (e.g., Hosen et al., 2019; Sun et al., 2016). Modeling results presented herein show that the dry

423   meteorological conditions are associated with relatively higher transpiration and ET$_a$ rates, similar to Zhao et al. (2022)

424   and Diao et al. (2021). During dry years, the increase in transpiration is positively correlated with higher NPP, which

425   in turn relates to lower relative ecosystem service water productivity values (Fig. 9).

426   In the SNW, green water use is higher in years with less than average precipitation. Accordingly, green water value

427   was highest, at $424.7 million (in CAD 2022), for the 2012 drought year (Fig. 10). It is important to note that value

428   of the subsurface water contribution is second highest, at 418.63 million, for 2016, which is also a drought year. Hence,

429   the critical role of subsurface water in sustaining ecosystem services is especially evident during both drought years

430   and more typical climatic conditions.

431   **4.3 Strengths and Limitations of Fully-Integrated GW-SW Models**

432   While the study herein advances the scientific utility of physics-based fully-integrated groundwater–surface water

433   models, it is essential to acknowledge the inherent uncertainty associated with such an analysis, along with factors

434   that could potentially reduce this uncertainty. It is well known that highly parameterized, structurally complex models

435   can have many degrees of freedom, high data requirements, and non-uniqueness challenges (Beven, 2006). However,

436   the parameterization of physics-based models can also be viewed as a strength due to the constraining relationship

437   between physically measurable characteristics and parameter values (Ebel and Loague, 2006). For the SNW, soil and

438   subsurface materials are well characterized and hence the spatial distribution and magnitudes of the associated

439   hydraulic parameters are generally well represented in the HGS model. Incorporating meteorological variability into

440   structurally complex model calibration and performance evaluation can also act to reduce uncertainty (Moeck et al.,

441   2018). Because the SNW simulation extended over an 18-year time frame that included multiple droughts and floods,

442   there is confidence that the model structure and parameterization is suited for a wide spectrum of hydrologic

443 conditions, and that the model can dynamically capture transitions from wet-to-dry and dry-to-wet conditions, which

444 is a critical part of the SNW analysis.

445 Fully-integrated groundwater - surface water models are ideally suited for the type of challenge addressed in the work

446 herein because simpler models lack process representation critical within the problem conceptualization (Ebel and

447 Loague, 2006). This is especially true when considering difficulties associated with quantifying large scale

448 evaporation and transpiration fluxes (Stoy et al., 2019), and groundwater–surface water interactions (Barthel and

449 Banzhaf, 2016). Structurally complex models have been shown to perform better than simple models when simulating

450 evapotranspiration (Ghasemizade et al., 2015) and groundwater recharge (Moeck et al., 2018), and previous work by

451 Hwang et al. (2015) demonstrated the utility of HGS for constraining ET at the watershed scale within the same

452 geographic region as the SNW. Further confidence in the SNW HGS model can be established through comparison

453 with other studies. In terms of overall water balance, results from the study herein compare closely with data compiled

454 as part of regional water management study encompassing the SNW (EOWRMS, 2001). Although the study time

455 frames differ (the EOWRMS (2001) study utilized pre-2000 data), the results are similar, with ETa accounting for

456 approximately 45 % and 62 % of annual precipitation in EOWRMS (2001) and the study herein, respectively. While

457 there is limited previous work investigating the partitioning of ETa into transpiration and evaporation that can be

458 directly compared, it is useful to refer to highly detailed analysis based off Fluxnet data (Pastorello et al., 2020) as

459 reference for transpiration and evaporation partitioning in landcover settings representative of those within the SNW.

460 For example, Xue et al. (2023) reported that transpiration as a percentage of ET ranged (depending on calculation

461 method) from 21-56 % and 39-83 % in Fluxnet data from cropland and mixed forest settings, respectively, whereas

462 the HGS model predicts an aggregate range of 45-65 % across the SNW watershed, which supports the use of HGS

463 transpiration estimates in subsequent ecosystem services valuation.

464 **4.4 Extension to Other Regions**

465 The methodology employed in this study provides a basis for deploying fully-integrated groundwater – surface water

466 models to assess subsurface water contribution to ecosystem services in other regions. However, it must be noted that

467 the results and values used herein are not necessarily transferable to other sites/watersheds. The marginal product of

468 water is a site-specific entity that will be different for other watersheds because both ecosystem services value and

469 transpiration rate will change in response to factors such as land cover, NPP, climate/weather, hydrogeology, and soil

470   properties. Nevertheless, given the ability of fully-integrated models to quantify the dynamic fluctuation in water

471   storages across different compartments, along with the linkage to terrestrial ecosystem services, the approach can be

472   expected to yield reliable results under similar workflow (modelling of water storages and transpiration rates, and

473   valuation of ecosystem services) for other locations/sites/watersheds.

474   **5 Conclusions**

475   This study characterizes and quantifies the important contribution of subsurface water towards sustaining ecosystem

476   services, which, until now has not been comprehensively studied. The prior lack of attention to subsurface water in

477   part relates to the complexities involved with characterizing the dynamic movement of water between subsurface

478   water and surface water storage compartments, and the related supply of green water. In the work herein, focusing on

479   a 3830 km^2 mixed use watershed, the innovative use of a HGS fully-integrated groundwater – surface water model for

480   water ecosystem services valuation is demonstrated, with the endpoint being monetization of the contributions of

481   subsurface water to green water supply over a period of 18 years (2000-2017). Results show that droughty conditions

482   are a major impetus for increased green water use. The maximum annual productive green water value was $424.7

483   million (CAD 2022) during the 2012 drought year, while the 18-year average was $338.83 million. Similarly, in other

484   dry years (i.e., 2001-2002 and 2016), there was a discernible rise in the green water use. Conversely, the results show

485   a notable decrease in the green water use during years characterized by higher precipitation, as exemplified in the year

486   2000 where green water provided $245.9 million in ecosystem services value. Hence, the study emphasizes the key

487   role of subsurface water in supplying green water and sustaining ecosystem services during critical periods when the

488   watershed is under meteorological drought.

489   Surface water ecosystem services are frequently valued in the literature, whereas the valuation of subsurface water

490   reserves and flows receives considerably less attention. Valuing groundwater resources can provide watershed

491   stewards incentives they can use to support land use management practices that influence flood damages, drought

492   impacts, drinking water quality/quantity, and ecological functions in surface water systems, for instance. The

493   valuation approach provided herein, using integrated numerical hydrogeological models, provides a rigorous

494   standardized means to provision value to ecosystem services associated with all components of the hydrological cycle.

495   This approach offers a template for standardizing water valuation in ecosystem service markets and could guide the

496   integration of water ecosystem service payments across diverse jurisdictions.

Author contribution

Tariq Aziz contributed to concept development, methodology, formal analysis, investigation, modelling, and writing the original draft.

Steven K. Frey contributed to concept development, methodology, data curation, HGS modeling, project administration, and reviewing and editing the manuscript.

David R. Lapen contributed to methodology development, reviewing and editing the manuscript, and project administration.

Susan Preston contributed to methodology development, reviewing and editing the manuscript, and project administration.

Hazen A. J. Russell contributed to hydrogeologic characterization, and with reviewing and editing the manuscript.

Omar Khader contributed to data curation, HGS model development, and formal analysis.

Andre R. Erler contributed to data curation and reviewing the manuscript.

Edward A. Sudicky contributed to project administration and reviewing the manuscript.

Declaration of interest

The authors declare that they have no known competing financial interests or personal relationships that could have appeared to influence the work reported in this paper.

References

Agriculture and Agri-Food Canada: Annual Space-Based Crop Inventory for Canada, 2017, Agroclimate, Geomatics and Earth Observation Division, Science and Technology Branch, 2017.

Allen, R. G., Pereira, L. S., Raes, D., and Smith, M.: Crop evapotranspiration guidelines for computing crop requirements, Rome, 1998.

An, S. and Verhoeven, J. T. A.: Wetlands: Ecosystem services, restoration and wise use, Springer, 325 pp., https://doi.org/10.1007/978-3-030-14861-4, 2019.

Aquanty: HydroGeoSphere: A three-dimensional numerical model describing fully-integrated subsurface and surface flow and solute transport, Waterloo, 2021.

Arnold, J. G., Srinivasan, R., Muttiah, R. S., and Williams, J. R.: Large area hydrologic modeling and assessment part I: Model development, J. Am. Water Resour. Assoc., 34, 73–89, https://doi.org/10.1111/j.1752-1688.1998.tb05961.x, 1998.

Aziz, T.: Changes in land use and ecosystem services values in Pakistan, 1950–2050, Environ. Dev., 35, 13, https://doi.org/10.1016/j.envdev.2020.100576, 2021.

Aziz, T., Nimubona, A.-D., and Cappellen, P. Van: Comparative Valuation of Three Ecosystem Services in a Canadian Watershed Using Global, Regional, and Local Unit Values, Sustainability, 15, 17, https://doi.org/ttps://doi.org/10.3390/su151411024, 2023.

Barthel, R. and Banzhaf, S.: Groundwater and Surface Water Interaction at the Regional-scale – A Review with Focus

531   on Regional Integrated Models, Water Resour. Manag., 30, 1–32, https://doi.org/10.1007/s11269-015-1163-z, 2016.

532   Berg, S. J. and Sudicky, E. A.: Toward Large-Scale Integrated Surface and Subsurface Modeling, Groundwater, 57,

533   1–2, https://doi.org/10.1111/gwat.12844, 2019.

534   Beven, K.: A manifesto for the equifinality thesis, J. Hydrol., 320, 18–36,

535   https://doi.org/10.1016/j.jhydrol.2005.07.007, 2006.

536   Bolte, J.: Envision integrated modeling platform, 94 pp., 2022.

537   Booth, E. G., Zipper, S. C., Loheide, S. P., and Kucharik, C. J.: Is groundwater recharge always serving us well?

538   Water supply provisioning, crop production, and flood attenuation in conflict in Wisconsin, USA, Ecosyst. Serv., 21,

539   153–165, 2016.

540   Brunner, P. and Simmons, C. T.: HydroGeoSphere: A Fully Integrated, Physically Based Hydrological Model, Ground

541   Water, 50, 170–176, https://doi.org/10.1111/j.1745-6584.2011.00882.x, 2012.

542   Casagrande, E., Recanati, F., Cristina, M., Bevacqua, D., and Meli, P.: Water balance partitioning for ecosystem

543   service assessment. A case study in the Amazon, Ecol. Indic., 121, https://doi.org/10.1016/j.ecolind.2020.107155,

544   2021.

545   Chen, X. and Hu, Q.: Groundwater influences on soil moisture and surface evaporation, J. Hydrol., 297, 285–300,

546   https://doi.org/10.1016/j.jhydrol.2004.04.019, 2004.

547   Condon, L. E., Atchley, A. L., and Maxwell, R. M.: Evapotranspiration depletes groundwater under warming over the

548   contiguous United States, Nat. Commun., 11, https://doi.org/10.1038/s41467-020-14688-0, 2020.

549   Costanza, R., D'Arge, R., De Groot, R., Farber, S., Grasso, M., Hannon, B., Limburg, K., Naeem, S., O'Neill, R. V.,

550   Paruelo, J., Raskin, R. G., Sutton, P., and Van Den Belt, M.: The value of ecosystem services: Putting the issues in

551   perspective, Ecol. Econ., 25, 67–72, https://doi.org/10.1016/S0921-8009(98)00019-6, 1998.

552   Cummings, D. I., Gorrell, G., Guilbault, J., Hunter, J. A., Logan, C., Pugin, A. J., Pullan, S. E., Russell, H. A. J., and

553   Sharpe, D. R.: Sequence stratigraphy of a glaciated basin fi ll , with a focus on esker sedimentation, Eol. Soc. Am.

554   Bull., 1478–1496, https://doi.org/10.1130/B30273.1, 2011.

555   Decsi, B., Ács, T., Jolánkai, Z., Kardos, M. K., Koncsos, L., Vári, Á., and Kozma, Z.: From simple to complex –

556   Comparing four modelling tools for quantifying hydrologic ecosystem services, Ecol. Indic., 141,

557   https://doi.org/10.1016/j.ecolind.2022.109143, 2022.

558   Dennedy-Frank, P. J., Muenich, R. L., Chaubey, I., and Ziv, G.: Comparing two tools for ecosystem service

559   assessments regarding water resources decisions, J. Environ. Manage., 177, 331–340,

560   https://doi.org/10.1016/j.jenvman.2016.03.012, 2016.

561   Diao, H., Wang, A., Yang, H., Yuan, F., Guan, D., and Wu, J.: Responses of evapotranspiration to droughts across

562   global forests: A systematic assessment, Can. J. For. Res., 51, 1–9, https://doi.org/10.1139/cjfr-2019-0436, 2021.

563   Ebel, B. A. and Loague, K.: Physics-based hydrologic-response simulation: Seeing through the fog of equifinality,

564   Hydrol. Process., 20, 2887–2900, https://doi.org/10.1002/hyp.6388, 2006.

565   Endsley, K. A., Zhao, M., Kimball, J., and Deva, S.: Continuity of global MODIS terrestrial primary productivity

566   estimates in the VIIRS era using model-data fusion, J. Geophys. Res. Biogeosciences,

567   https://doi.org/10.22541/essoar.167768101.16068273/v1, 2023.

568   EOWRMS: Eastern Ontario water resources management study (final report), Ottawa, Ontario, 5–24 pp., 2001.

569   Erler, A. R., Frey, S. K., Khader, O., d'Orgeville, M., Park, Y. J., Hwang, H. T., Lapen, D. R., Richard Peltier, W.,

570   and Sudicky, E. A.: Simulating Climate Change Impacts on Surface Water Resources Within a Lake-Affected Region

571   Using Regional Climate Projections, Water Resour. Res., 55, 130–155, https://doi.org/10.1029/2018WR024381,

572   2019.

573   Foster, S. S. D. and Chilton, P. J.: Groundwater: The processes and global significance of aquifer degradation, Philos.

574   Trans. R. Soc. B Biol. Sci., 358, 1957–1972, https://doi.org/10.1098/rstb.2003.1380, 2003.

575   Frey, S. K., Miller, K., Khader, O., Taylor, A., Morrison, D., Xu, X., Berg, S. J., Sudicky, E. A., and Lapen, D. R.:

576   Evaluating landscape influences on hydrologic behavior with a fully- integrated groundwater – surface water model,

577   J. Hydrol., 602, 1–8, 2021.

578   Ghasemizade, M., Moeck, C., and Schirmer, M.: The effect of model complexity in simulating unsaturated zone flow

579   processes   on   recharge   estimation   at   varying   time   scales,   J.   Hydrol.,   529,   1173–1184,

580   https://doi.org/10.1016/j.jhydrol.2015.09.027, 2015.

581   Griebler, C. and Avramov, M.: Groundwater ecosystem services: A review, Freshw. Sci., 34, 355–367,

582   https://doi.org/10.1086/679903, 2015.

583   Hogg, E. H.: Temporal scaling of moisture and the forest-grassland boundary in western Canada, Agric. For.

584   Meteorol., 84, 115–122, https://doi.org/10.1016/S0168-1923(96)02380-5, 1997.

585   Honeck, E., Gallagher, L., von Arx, B., Lehmann, A., Wyler, N., Villarrubia, O., Guinaudeau, B., and Schlaepfer, M.

586   A.: Integrating ecosystem services into policymaking – A case study on the use of boundary organizations, Ecosyst.

587   Serv., 49, https://doi.org/10.1016/j.ecoser.2021.101286, 2021.

588   Hosen, J. D., Aho, K. S., Appling, A. P., Creech, E. C., Fair, J. H., Hall, R. O., Kyzivat, E. D., Lowenthal, R. S., Matt,

589   S., Morrison, J., Saiers, J. E., Shanley, J. B., Weber, L. C., Yoon, B., and Raymond, P. A.: Enhancement of primary

590   production during drought in a temperate watershed is greater in larger rivers than headwater streams, Limnol.

591   Oceanogr., 64, 1458–1472, https://doi.org/10.1002/lno.11127, 2019.

592   Hwang, H. T., Park, Y. J., Frey, S. K., Berg, S. J., and Sudicky, E. A.: A simple iterative method for estimating

593   evapotranspiration   with   integrated   surface/subsurface   flow   models,   J.   Hydrol.,   531,   949–959,

594   https://doi.org/10.1016/j.jhydrol.2015.10.003, 2015.

595   Jin, Z., Liang, W., Yang, Y., Zhang, W., Yan, J., Chen, X., Li, S., and Mo, X.: Separating Vegetation Greening and

596   Climate   Change   Controls   on   Evapotranspiration   trend   over   the   Loess   Plateau,   Sci.   Rep.,   7,   1–15,

597   https://doi.org/10.1038/s41598-017-08477-x, 2017.

598   Kollet, S., Mauro, S., M., M. R., Paniconi, C., Putti, M., Bertoldi, G., Coon, E. T., Cordano, E., Endrizzi, S., Kikinzon,

599   E., Mouche, E., M€ugler, C., Park, Y.-J., Refsgaard, J. C., Stisen, S., and Sudicky, E.: The integrated hydrologic model

600   intercomparison project, IH-MIP2: A second set of benchmark results to diagnose integrated hydrology and feedbacks,

601   Water Resour. Res., 867–890, https://doi.org/10.1002/2016WR019191.Received, 2016.

602   Kornelsen, K. C. and Coulibaly, P.: Synthesis review on groundwater discharge to surface water in the Great Lakes

603   Basin, J. Great Lakes Res., 40, 247–256, https://doi.org/10.1016/j.jglr.2014.03.006, 2014.

604   L'Ecuyer-Sauvageau, C., Dupras, J., He, J., Auclair, J., Kermagoret, C., and Poder, T. G.: The economic value of

605   Canada's National Capital Green Network, PLoS One, 16, 1–29, https://doi.org/10.1371/journal.pone.0245045, 2021.

606   Li, Q., Qi, J., Xing, Z., Li, S., Jiang, Y., Danielescu, S., Zhu, H., Wei, X., and Meng, F. R.: An approach for assessing

607   impact of land use and biophysical conditions across landscape on recharge rate and nitrogen loading of groundwater,

608   Agric. Ecosyst. Environ., 196, 114–124, https://doi.org/10.1016/j.agee.2014.06.028, 2014.

609   Liang, X., Lettenmaier, D. P., Wood, E. F., and Burges, S. J.: A simple hydrologically based model of land surface

610   water and energy fluxes for general circulation models, J. Geophys. Res., 99, https://doi.org/10.1029/94jd00483, 1994.

611   Liu, Y. and El-Kassaby, Y. A.: Evapotranspiration and favorable growing degree-days are key to tree height growth

612   and ecosystem functioning: Meta-Analyses of Pacific Northwest historical data, 1st Annu. IEEE Conf. Control

613   Technol. Appl. CCTA 2017, 2017-Janua, 7–12, https://doi.org/10.1038/s41598-018-26681-1, 2017.

614   Liu, Y., Zhou, R., Wen, Z., Khalifa, M., Zheng, C., Ren, H., Zhang, Z., and Wang, Z.: Assessing the impacts of

615   drought on net primary productivity of global land biomes in different climate zones, Ecol. Indic., 130, 108146,

616   https://doi.org/10.1016/j.ecolind.2021.108146, 2021.

617   Logan, C., Cummings, D. I., Pullan, S., Pugin, A., Russell, H. A. J., and Sharpe, D. R.: Hydrostratigraphic model of

618   the South Nation watershed region, south-eastern Ontario, Geological Survey of Canada, 17 pp.,

619   https://doi.org/https://doi.org/10.4095/248203, 2009.

620   Loheide, S. P.: A method for estimating subdaily evapotranspiration of shallow groundwater using diurnal water table

621   fluctuations, Ecohydrology, 1, 59–66, 2008.

622   Lowe, B. H., Zimmer, Y., and Oglethorpe, D. R.: Estimating the economic value of green water as an approach to

623   foster the virtual green-water trade, Ecol. Indic., 136, 108632, https://doi.org/10.1016/j.ecolind.2022.108632, 2022.

624   Mammola, S., Cardoso, P., Culver, D. C., Deharveng, L., Ferreira, R. L., Fišer, C., Galassi, D. M. P., Griebler, C.,

625   Halse, S., Humphreys, W. F., Isaia, M., Malard, F., Martinez, A., Moldovan, O. T., Niemiller, M. L., Pavlek, M.,

626   Reboleira, A. S. P. S., Souza-Silva, M., Teeling, E. C., Wynne, J. J., and Zagmajster, M.: Scientists' warning on the

627   conservation of subterranean ecosystems, Bioscience, 69, 641–650, https://doi.org/10.1093/biosci/biz064, 2019.

628   Maxwell, R. M., Putti, M., Meyerhoff, S., Delfs, J.-O., Ferguson, I. M., Ivanov, V., Jongho Kim, O. K., Stefan J.

629   Kollet, M. K., Lopez, S., Jie Niu, Claudio Paniconi, Y.-J. P., Mantha S. Phanikumar, C. S., Sudicky, E. A., and Sulis,

630   M.: Surface-subsurface model intercomparison: A first set of benchmark results to diagnose integrated hydrology and

631   feedbacks, Water Resour. Res., 1531–1549, https://doi.org/10.1002/2013WR013725.Received, 2014.

632   McKenney, D. W., Hutchiinson, M. F., Papadopol, P., Lawrence, K., Pedlar, J., Campbell, K., Milewska, E.,

633   Hopkinson, R. F., Price, D., and Owen, T.: Customized spatial climate models for North America, Bull. Am. Meteorol.

634   Soc., 92, 1611–1622, https://doi.org/10.1175/2011BAMS3132.1, 2011.

635   Mercado-bettín, D., Salazar, J. F., and Villegas, J. C.: Long-term water balance partitioning explained by physical and

636   ecological characteristics in world river basins, Ecohydrology, 12, 1–13,

637   https://doi.org/https://doi.org/10.1002/eco.2072, 2019.

638   Millenium Ecosystem Assessment (MEA): Ecosystems and Human Well-Being: Synthesis, Island Press, 285 pp.,

639   https://doi.org/10.1057/9780230625600, 2005.

640   Moeck, C., von Freyberg, J., and Schirmer, M.: Groundwater recharge predictions in contrasted climate: The effect of

641   model complexity and calibration period on recharge rates, Environ. Model. Softw., 103, 74–89,

https://doi.org/10.1016/j.envsoft.2018.02.005, 2018.

Moriasi, D. N., Arnold, J. G., Van Liew, M. W., Bingner, R. L., Harmel, R. D., and Veith, T. L.: Model evaluation guidelines for systematic quantification of accuracy in watershed simulations, Trans. ASABE, 50, 885–900, https://doi.org/10.13031/2013.23153, 2007.

Mulligan, M.: User guide for the Co$ting Nature Policy Support System v.2., https://goo.gl/Grpbnb, 2015.

Muñoz-Sabater, J., Dutra, E., Agustí-Panareda, A., Albergel, C., Arduini, G., Balsamo, G., Boussetta, S., Choulga, M., Harrigan, S., Hersbach, H., Martens, B., Miralles, D. G., Piles, M., Rodríguez-Fernández, N. J., Zsoter, E., Buontempo, C., and Thépaut, J. N.: ERA5-Land: A state-of-the-art global reanalysis dataset for land applications, Earth Syst. Sci. Data, 13, 4349–4383, https://doi.org/10.5194/essd-13-4349-2021, 2021.

MYD15A2H MODIS/Aqua Leaf Area Index/FPAR 8-Day L4 Global 500m SIN Grid. NASA LP DAAC:

Natural Capital Project: InVEST User Guide 3.12.0, 1–7 pp., 2022.

Neff, B. P., Day, S. M., Piggott, A. R., and Fuller, L. M.: Base flow in the Great Lakes basin, U.S. Geol. Surv. Sci. Investig. Rep., 32, 2005.

Ochoa, V. and Urbina-Cardona, N.: Tools for spatially modeling ecosystem services: Publication trends, conceptual reflections and future challenges, Ecosyst. Serv., 26, 155–169, https://doi.org/10.1016/j.ecoser.2017.06.011, 2017.

Ontario Geological Survey: Surficial Geology of Southern Ontario, Miscellaneous Release--Data 128-REV. Ontario Geological Survey., 1–7 pp., 2010.

Ontario Integrated Hydrology Data: https://geohub.lio.gov.on.ca/maps/mnrf::ontario-integrated-hydrology-oih-data/about.

Pastorello, G., Trotta, C., Canfora, E., Chu, H., Christianson, D., Cheah, Y. W., Poindexter, C., Chen, J., Elbashandy, A., Humphrey, M., Isaac, P., Polidori, D., Ribeca, A., van Ingen, C., Zhang, L., Amiro, B., Ammann, C., Arain, M. A., Ardö, J., Arkebauer, T., Arndt, S. K., Arriga, N., Aubinet, M., Aurela, M., Baldocchi, D., Barr, A., Beamesderfer, E., Marchesini, L. B., Bergeron, O., Beringer, J., Bernhofer, C., Berveiller, D., Billesbach, D., Black, T. A., Blanken, P. D., Bohrer, G., Boike, J., Bolstad, P. V., Bonal, D., Bonnefond, J. M., Bowling, D. R., Bracho, R., Brodeur, J., Brümmer, C., Buchmann, N., Burban, B., Burns, S. P., Buysse, P., Cale, P., Cavagna, M., Cellier, P., Chen, S., Chini, I., Christensen, T. R., Cleverly, J., Collalti, A., Consalvo, C., Cook, B. D., Cook, D., Coursolle, C., Cremonese, E., Curtis, P. S., D'Andrea, E., da Rocha, H., Dai, X., Davis, K. J., De Cinti, B., de Grandcourt, A., De Ligne, A., De Oliveira, R. C., Delpierre, N., Desai, A. R., Di Bella, C. M., di Tommasi, P., Dolman, H., Domingo, F., Dong, G., Dore, S., Duce, P., Dufrêne, E., Dunn, A., Dušek, J., Eamus, D., Eichelmann, U., ElKhidir, H. A. M., Eugster, W., Ewenz, C. M., Ewers, B., Famulari, D., Fares, S., Feigenwinter, I., Feitz, A., Fensholt, R., Filippa, G., Fischer, M., Frank, J., Galvagno, M., Gharun, M., Gianelle, D., et al.: The FLUXNET2015 dataset and the ONEFlux processing pipeline for eddy covariance data, Sci. Data, 7, 1–27, https://doi.org/10.1038/s41597-020-0534-3, 2020.

Qiu, J., Zipper, S. C., Motew, M., Booth, E. G., Kucharik, C. J., and Loheide, S. P.: Nonlinear groundwater influence on biophysical indicators of ecosystem services, Nat. Sustain., 2, 475–483, https://doi.org/10.1038/s41893-019-0278-2, 2019.

Richardson, M. and Kumar, P.: Critical Zone services as environmental assessment criteria in intensively managed landscapes, Earth's Futur., 5, 617–632, https://doi.org/10.1002/2016EF000517, 2017.

679   Schaap, M. G., Leij, F. J., and Van Genuchten, M. T.: Rosetta: A computer program for estimating soil hydraulic

680   parameters with hierarchical pedotransfer functions, J. Hydrol., 251, 163–176, https://doi.org/10.1016/S0022-

681   1694(01)00466-8, 2001.

682   Schyns, J. F., Hoekstra, A. Y., Booij, M. J., Hogeboom, R. J., and Mekonnen, M. M.: Limits to the world's green

683   water resources for food, feed, fiber, timber, and bioenergy, Proc. Natl. Acad. Sci. U. S. A., 116, 4893–4898,

684   https://doi.org/10.1073/pnas.1817380116, 2019.

685   Siebert, S., Burke, J., Faures, J. M., Frenken, K., Hoogeveen, J., Döll, P., and Portmann, F. T.: Groundwater use for

686   irrigation - A global inventory, Hydrol. Earth Syst. Sci., 14, 1863–1880, https://doi.org/10.5194/hess-14-1863-2010,

687   2010.

688   SLC: Soil Landscapes of Canada Version 3.2, 2007–2008 pp., 2010.

689   Stoy, P. C., El-Madany, T. S., Fisher, J. B., Gentine, P., Gerken, T., Good, S. P., Klosterhalfen, A., Liu, S., Miralles,

690   D. G., Perez-Priego, O., Rigden, A. J., Skaggs, T. H., Wohlfahrt, G., Anderson, R. G., Coenders-Gerrits, A. M. J.,

691   Jung, M., Maes, W. H., Mammarella, I., Mauder, M., Migliavacca, M., Nelson, J. A., Poyatos, R., Reichstein, M.,

692   Scott, R. L., and Wolf, S.: Reviews and syntheses: Turning the challenges of partitioning ecosystem evaporation and

693   transpiration into opportunities, Biogeosciences, 16, 3747–3775, https://doi.org/10.5194/bg-16-3747-2019, 2019.

694   Su, Y., Feng, Q., Zhu, G., Wang, Y., and Zhang, Q.: A New Method of Estimating Groundwater Evapotranspiration

695   at   Sub-Daily   Scale   Using   Water   Table   Fluctuations,   Water   (Switzerland),   14,   1–14,

696   https://doi.org/10.3390/w14060876, 2022.

697   Sun, B., Zhao, H., and Wang, X.: Effects of drought on net primary productivity: Roles of temperature, drought

698   intensity, and duration, Chinese Geogr. Sci., 26, 270–282, https://doi.org/10.1007/s11769-016-0804-3, 2016.

699   Sun, G., Hallema, D., and Asbjornsen, H.: Ecohydrological processes and ecosystem services in the Anthropocene: a

700   review, Ecol. Process., 6, https://doi.org/10.1186/s13717-017-0104-6, 2017.

701   Tan, S., Wang, H., Prentice, I. C., and Yang, K.: Land-surface evapotranspiration derived from a first-principles

702   primary production model, Environ. Res. Lett., 16, https://doi.org/10.1088/1748-9326/ac29eb, 2021.

703   Vigerstol, K. L. and Aukema, J. E.: A comparison of tools for modeling freshwater ecosystem services, J. Environ.

704   Manage., 92, 2403–2409, https://doi.org/10.1016/j.jenvman.2011.06.040, 2011.

705   Villa, F., Bagstad, K., and Balbi, S.: ARIES: Artificial Intelligence for Environment & Sustainability, 2021.

706   Wheaton, E., Kulshreshtha, S., Wittrock, V., and Koshida, G.: Dry times: Hard lessons from the Canadian drought of

707   2001 and 2002, Can. Geogr., 52, 241–262, https://doi.org/10.1111/j.1541-0064.2008.00211.x, 2008.

708   Xu, C., Li, Y., Hu, J., Yang, X., Sheng, S., and Liu, M.: Evaluating the difference between the normalized difference

709   vegetation index and net primary productivity as the indicators of vegetation vigor assessment at landscape scale,

710   Environ. Monit. Assess., 184, 1275–1286, https://doi.org/10.1007/s10661-011-2039-1, 2012.

711   Xu, S., Frey, S. K., Erler, A. R., Khader, O., Berg, S. J., Hwang, H. T., Callaghan, M. V., Davison, J. H., and Sudicky,

712   E. A.: Investigating groundwater-lake interactions in the Laurentian Great Lakes with a fully-integrated surface water-

713   groundwater model, J. Hydrol., 594, 125911, https://doi.org/10.1016/j.jhydrol.2020.125911, 2021.

714   Xu, Y. and Xiao, F.: Assessing Changes in the Value of Forest Ecosystem Services in Response to Climate Change

715   in China, Sustain., 14, https://doi.org/10.3390/su14084773, 2022.

Xue, K., Song, L., Xu, Y., Liu, S., Zhao, G., Tao, S., Magliulo, E., Manco, A., Liddell, M., Wohlfahrt, G., Varlagin, A., Montagnani, L., Woodgate, W., Loubet, B., and Zhao, L.: Estimating ecosystem evaporation and transpiration using a soil moisture coupled two-source energy balance model across FLUXNET sites, Agric. For. Meteorol., 337, 1–7, https://doi.org/10.1016/j.agrformet.2023.109513, 2023.

Yang, H., Luo, P., Wang, J., Mou, C., Mo, L., Wang, Z., Fu, Y., Lin, H., Yang, Y., and Bhatta, L. D.: Ecosystem evapotranspiration as a response to climate and vegetation coverage changes in Northwest Yunnan, China, PLoS One, 10, 1–17, https://doi.org/10.1371/journal.pone.0134795, 2015.

Yang, X. and Liu, J.: Assessment and valuation of groundwater ecosystem services: A case study of Handan City, China, Water (Switzerland), 12, https://doi.org/10.3390/w12051455, 2020.

Yu, S., Miao, C., Song, H., Huang, Y., and Chen, W.: Efficiency of nitrogen and phosphorus removal by six macrophytes from eutrophic water Efficiency of nitrogen and phosphorus removal by six macrophytes from eutrophic water, Int. J. Phytoremediation, 21, 643–651, https://doi.org/10.1080/15226514.2018.1556582, 2019.

Zhang, T., Xu, M., Zhang, Y., Zhao, T., An, T., Li, Y., Sun, Y., Chen, N., Zhao, T., Zhu, J., and Yu, G.: Grazing-induced increases in soil moisture maintain higher productivity during droughts in alpine meadows on the Tibetan Plateau, Agric. For. Meteorol., 269–270, 249–256, https://doi.org/10.1016/j.agrformet.2019.02.022, 2019.

Zhao, M., Aa, G., Liu, Y., and Konings, A.: Evapotranspiration frequently increases during droughts, Nat. Clim. Chang., 12, 1024–1030, https://doi.org/https://doi.org/10.1038/s41558-022-01505-3, 2022.

Zisopoulou, K., Zisopoulos, D., and Panagoulia, D.: Water Economics: An In-Depth Analysis of the Connection of Blue Water with Some Primary Level Aspects of Economic Theory I, Water (Switzerland), 14, https://doi.org/10.3390/w14010103, 2022.

Appendix

The annual outputs (ET_a, surface water, subsurface water, precipitation and outflow) from the HGS model are given in Table A1.

Table A1: HGS outputs from the SNW simulation

Year	ETₐ (m³)	Surface water (m³)	Subsurface water (m³)	Precipitation (m³)	Outflow (m³)	Surface evaporation (m³)	Subsurface evaporation (m³)	Subsurface transpiration (m³)
2000	2,085,534,445	69,424,628	222,709,069,460	4,199,527,096	2,513,014,025	75,020,473	184,374,990	945,999,818
2001	2,477,004,097	54,513,422	222,240,461,950	3,003,497,233	1,229,179,146	49,049,150	193,684,126	1,525,263,969
2002	2,309,984,877	61,588,887	222,788,771,412	3,598,706,939	1,676,367,040	49,496,381	137,246,184	150,943,1,700
2003	2,264,696,091	68,998,342	222,524,086,305	4,253,877,105	2,171,628,188	63,041,934	155,345,628	1,263,073,935
2004	2,197,974,479	67,358,376	222,569,571,666	3,631,932,688	1,789,088,452	56,472,059	186,217,551	1,224,545,264
2005	2,416,958,064	67,153,617	222,566,818,892	3,988,298,138	1,933,741,551	62,293,999	203,745,742	1407,718,083
2006	2,293,950,204	74,422,486	222,666,754,361	4,538,849,536	2,510,031,879	73,310,604	176,406,194	1,175,390,417
2007	2,385,260,383	65,967,543	222,611,557,149	3,679,748,277	1,804,665,208	55,442,956	193,054,015	1,352,247,667
2008	2,236,139,918	79,130,070	222,736,726,608	5,070,858,236	3,028,106,623	63,243,999	153,505,172	1,001,912,242
2009	2,142,956,266	72,673,133	222,733,824,127	3,753,041,839	2,207,758,076	74,320,182	175,808,767	1,034,718,786
2010	2,450,480,102	67,043,193	222,626,541,197	3,686,832,140	1,818,134,266	78,166,506	204,928,373	1,337,194,629
2011	2,398,275,129	63,710,702	222,487,837,813	3,743,641,761	1,860,099,758	56,432,877	170,459,783	1,404,943,119

2012	2,589,094,745	52,013,667	222,334,569,769	2,864,258,811	951,529,742	58,974,276	223,348,145	1,633,465,101
2013	2,269,228,484	64,978,113	222,458,625,710	3,700,833,331	1,683,228,427	67,961,698	205,253,614	1,227,712,022
2014	2,193,041,030	69,944,514	222,574,462,508	3,974,971,693	2,057,632,005	67,115,318	170,740,982	1,220,179,455
2015	2,449,702,370	62,201,787	222,466,595,816	3,374,434,139	1,324,157,589	64,640,268	227,937,634	1,407,052,424
2016	2,516,780,613	59,120,794	222,402,665,868	3,747,442909	1,659,895,299	53,448,526	220,313,313	1,610,087,162
2017	2,273,903,311	80,775,412	222,688,809,435	5,228,987,865	3,333,168,400	77,841,432	192,369,477	1,176,497,385

The SNW has approximately 110 m of vertical relief from its highest point in the southwest corner to its outlet at the Ottawa

745   River at its northern edge (Fig. A1).
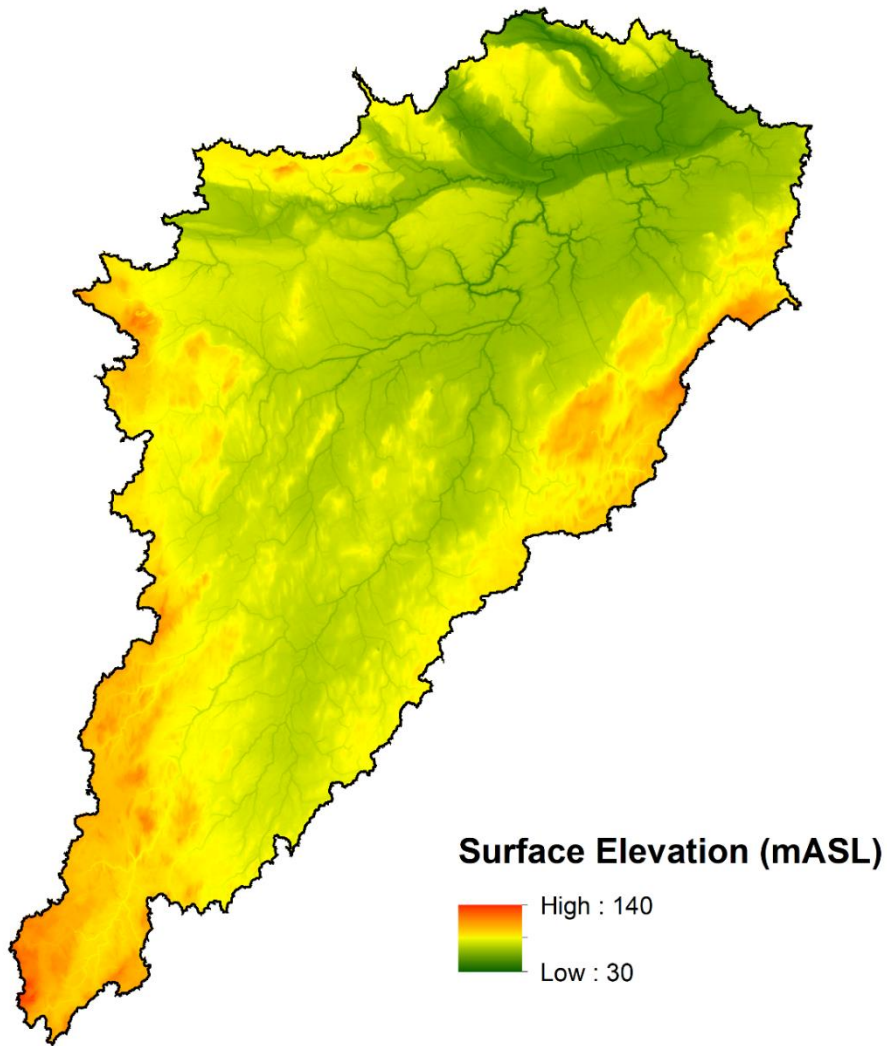
Figure A1: Land surface elevation of the SNW (Ontario Integrated Hydrology Data).
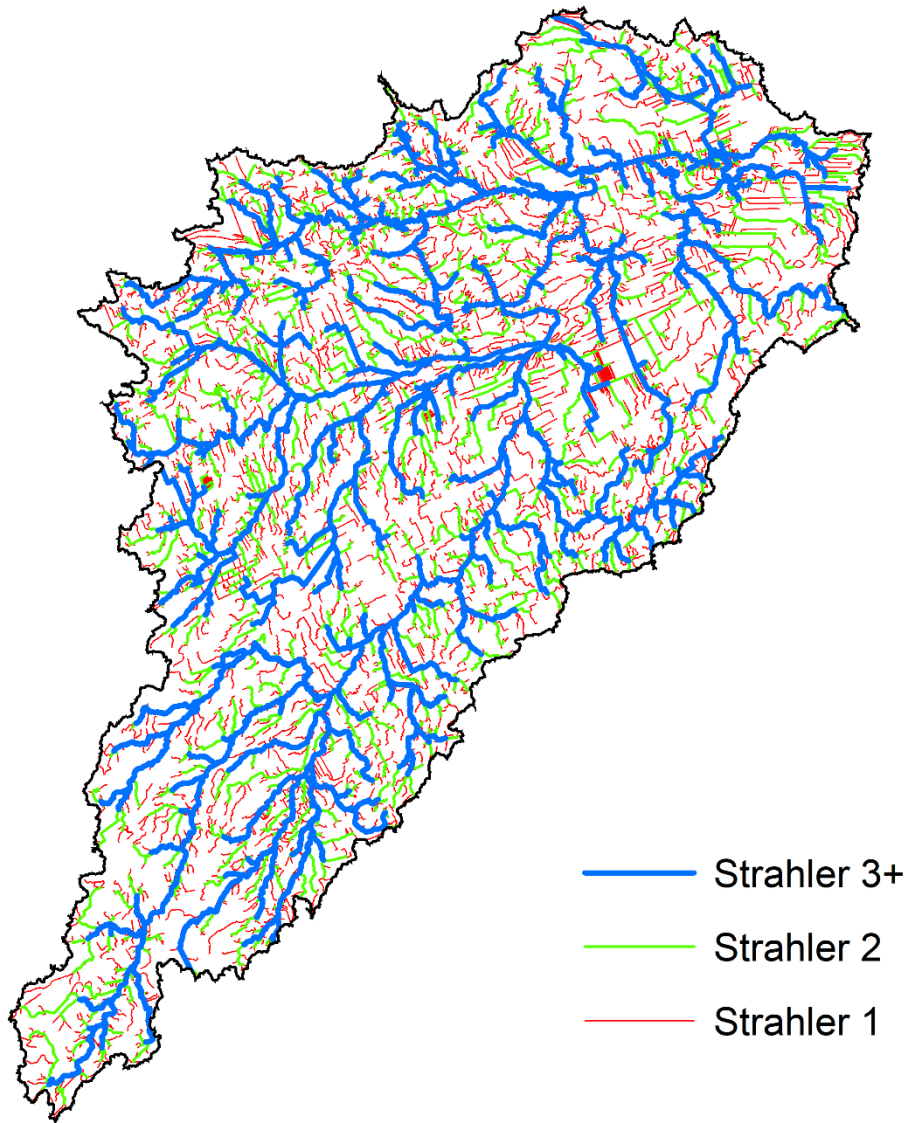
750

Figure A2. Stream network distribution across the South Nation watershed, consisting of 1606 km of Strahler 3+ streams, 1548

km of Strahler 2 streams, and 3335 km of Strahler 1 streams (Ontario Ministry of Natural Resources and Forestry 2013).
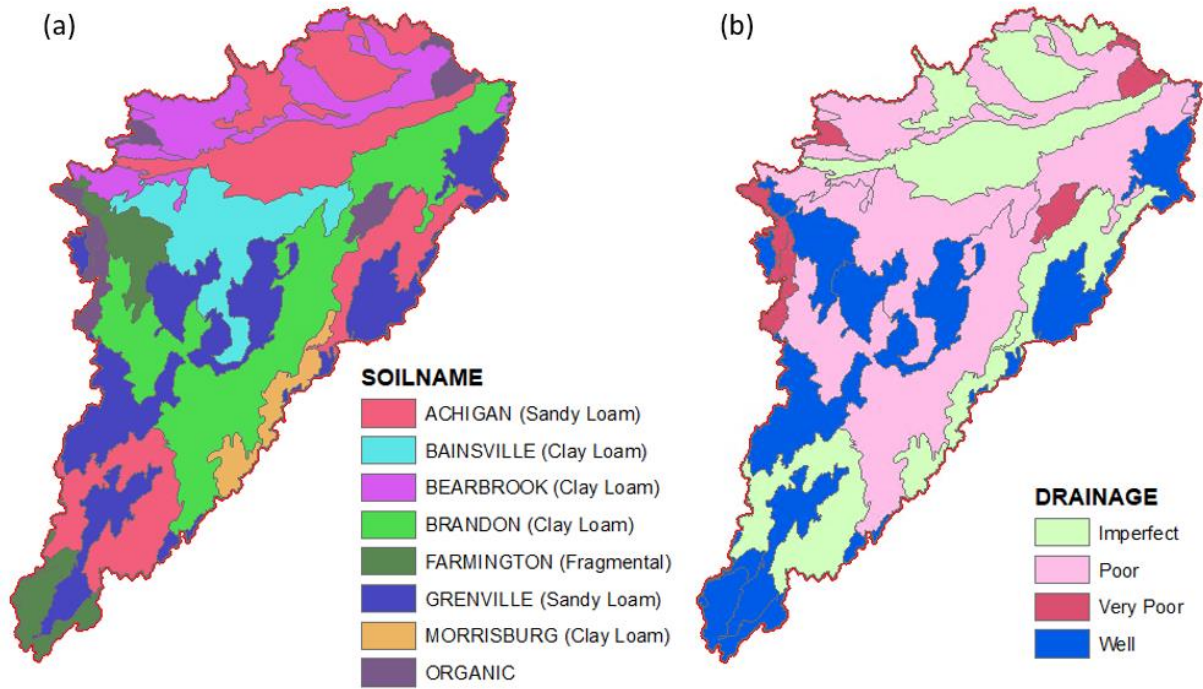
Figure A3. (a) Soil distribution, and (b) soil drainage status across the South Nation watershed (SLC, 2010) .
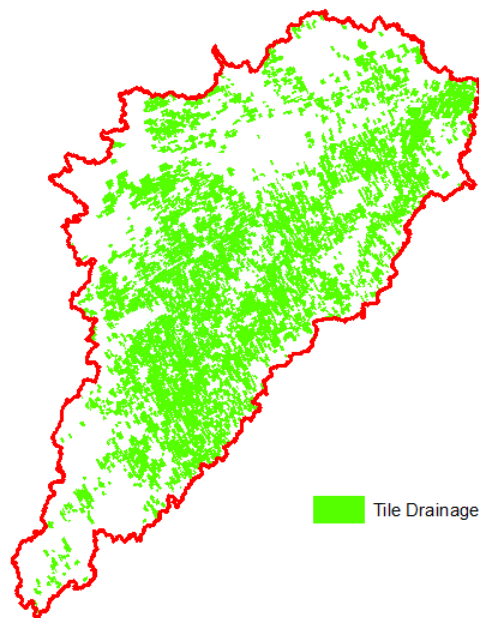
755

Figure A4. Tile drainage distribution across the South Nation watershed (data provided by the South Nation Conservation

Authority).
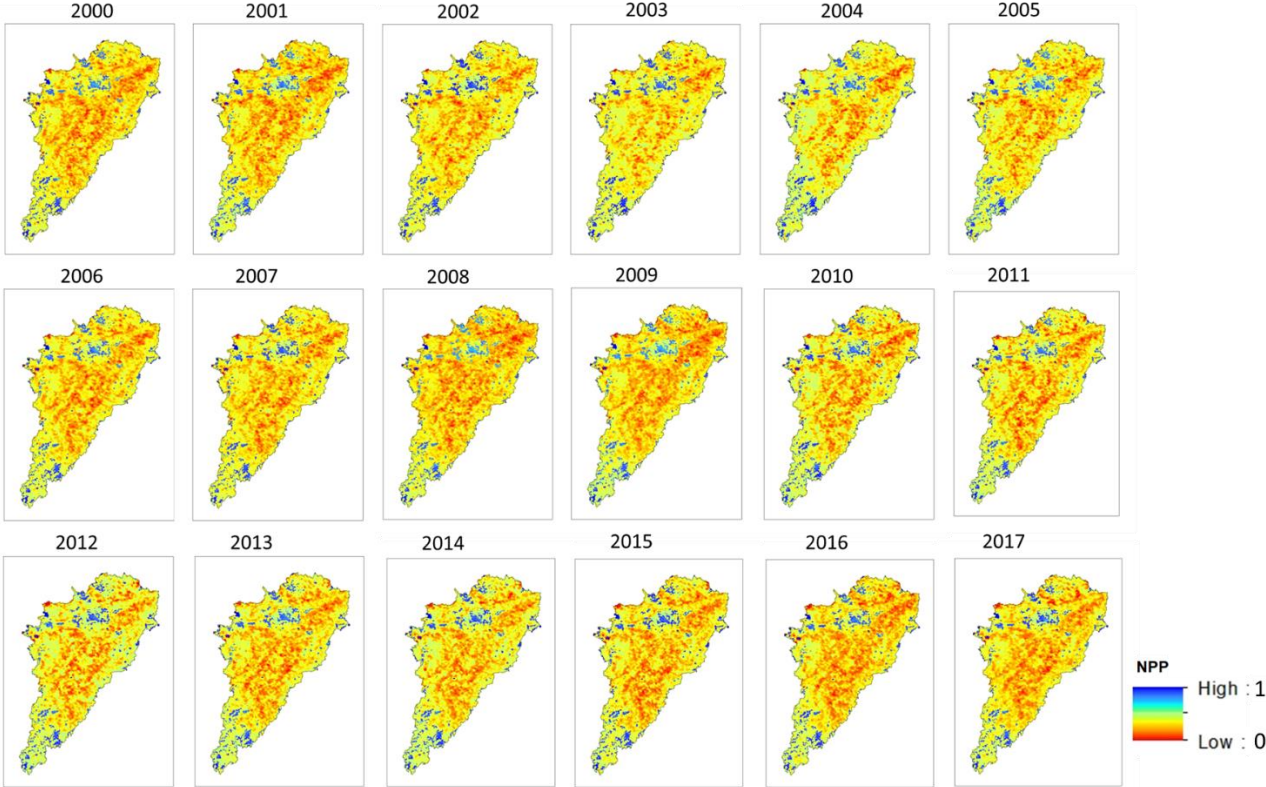
Figure A5: Net Primary Productivity (NPP) data for SNW (based on MODIS data (Endsley et al., 2023))